Effect of spacers on axial capacity of cold-formed steel back-to-back gapped channel sections

Seshagiri Rao Divi

A thesis submitted in fulfilment of the requirements

for the degree of Master of Engineering

Supervised by

Dr Zhiyuan (Arthur) Fang, Dr Krishanu Roy, and Prof James Lim

School of Engineering

The University of Waikato

New Zealand

2024

ABSTRACT

The use of cold-formed steel (CFS) gapped back-to-back channel sections is becoming popular, especially in New Zealand and South-East Asia. Introducing a gap between the back-to-back channels enhances resistance to lateral-torsional buckling. Previous research has investigated gapped built-up channel sections with spacers but hasn't determined the optimal number of spacers relative to length. Also, little attention has been given to how transverse spacing affects the axial capacity of these sections. This study fills those gaps by developing and validating a non-linear elastoplastic finite element (FE) model against experimental data. A parametric study of 1000 FE models examine the effects of column length, CFS section thickness, materials properties, and spacer spacing, on the axial capacity of gapped built-up columns. Key findings include: (1) Up to a column length of 4000 mm, three equally spaced spacers optimize compressive strength in gapped sections. (2) Optimal transverse spacing aligns with the channel web depth, offering no significant strength increase beyond 1.5 times the web depth. (3) Gapped sections show a substantial average increase (424%) in compressive strength over single-channel configurations, and a moderate improvement (125%) compared to non-gapped built-up sections. (4) FEA results closely match the predictions of AS/NZS-4600:2018, differing by only 5% in compressive strength.

Keywords: cold-formed steel, channel-section, gapped back-to-back sections, built-up gapped sections, spacers.

PREFACE

This thesis is submitted to the University of Waikato, New Zealand, in fulfilment of the requirement for the master's degree in civil engineering. The work in this thesis has not been previously submitted for a degree or diploma at any other higher educational institution. To the best of my knowledge and belief, the thesis contains no material previously published or written by another person except where due reference is made.

ACKNOWLEDGEMENTS

Firstly, my sincere thanks to my main supervisor, Dr Zhiyuan (Arthur) Fang, co-supervisors Dr Krishanu Roy, and Professor James B.P. Lim, for their unwavering support throughout my research, whose constant guidance and contributions were integral to the successful submission of my journal paper, making me an independent researcher.

Heartfelt gratitude goes to Shubham Tiwari, Vivekanandan Sivaji, Bikram Paul, and Kushal Gosh for their continuous support. I sincerely thank my well-wishers in New Zealand for shaping my thesis with invaluable encouragement.

I express my appreciation to my best friends in New Zealand, Shubham Tiwari, Vivekanandan Sivaji, Dinesh Lakshmanan Chandramohan, Gagan Sengundham, and Gowrava Mohanswamy for their year-round support. Special thanks to the University of Waikato, School of Engineering, for providing computing machines and research assistance.

Finally, I want to thank my family, my father Anjaneyulu Divi, my mother Annapoorna Divi, and my spouse Sirisha Devi Ponnuri for their unwavering support in pursuing my master's.

TABLE OF CONTENTS

LIST OF FIGURES

LIST OF TABLES

CHAPTER 1. Introduction

1.1 General

Cold-formed steel (CFS) structures, including roof trusses (see Figure 1-1), wall frames, and portal frames, are increasingly employing back-to-back gapped built-up CFS channel sections for column members. This design utilizes intermediate fasteners at specific intervals to prevent individual channel sections from buckling independently. However, there is a scarcity of experimental tests or finite element analyses in the literature that investigate the influence of longitudinal screw spacing on the axial capacity of these sections.

Figure 1-1: Practical application of Back-to-Back gapped sections in roof truss.

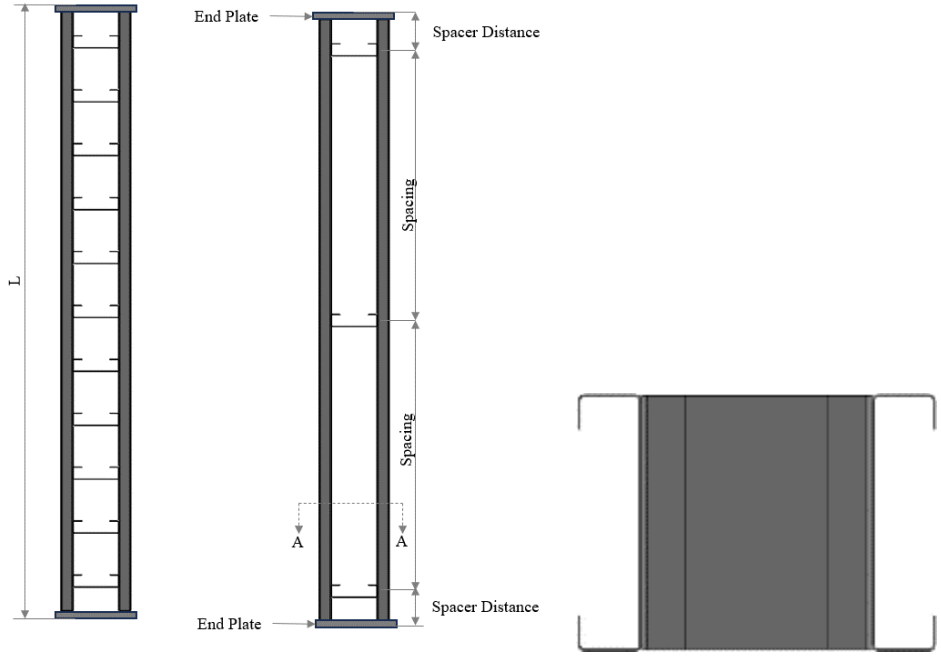

(a) General Arrangement (b) Section A-A

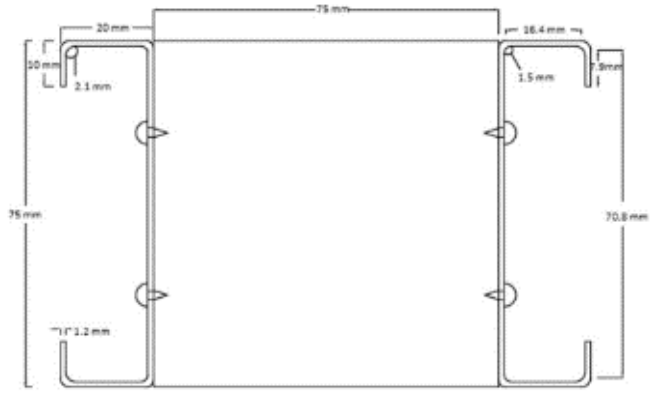

(c) GBU75

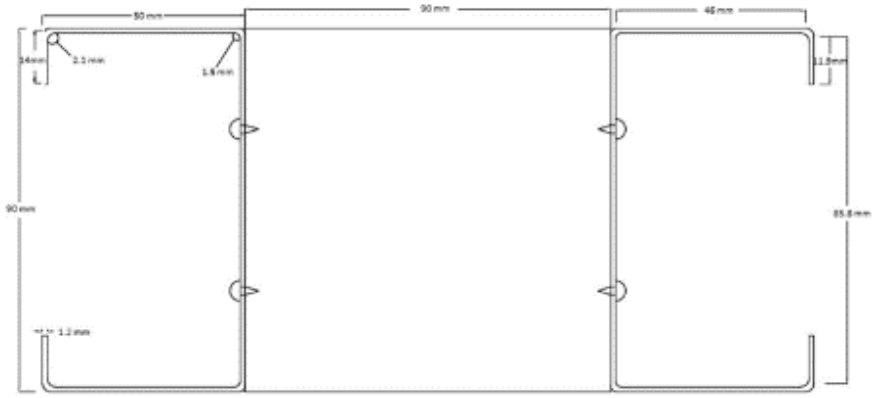

(d) GBU90

Figure 1-2: **(a)&(b)** Studies in literature using a greater number of spacers and the present study investigating the viability of a lesser number of spacers. **(c) &(d)** Nominal cross-sections of back-to-back gapped built-up cold-formed steel channel sections are considered in this paper by Roy et al [26]

Researchers have extensively studied the behavior of CFS built-up columns through both experimental and numerical investigations, focusing on utilizing channel and angle sections. However, the full potential of back-to-back gapped built-up channel sections is often underutilized due to insufficient transverse spacing. Introducing adequate spacing significantly enhances column performance by improving stability and reducing slenderness. Studies incorporating transverse spacing between channel sections, connected through webs and battens, have demonstrated strength improvements [25][26]. However, large transverse spacing between the channel sections and connected using battens greatly improved the axial strength behaviour of CFS built-up battened columns, especially when web-stiffened channels were adopted [46]. Nevertheless, challenges persist, particularly in addressing sectional buckling governed by the channel web's compactness.

To address these issues, there is a need to develop built-up sections where channel sections are appropriately spaced and connected through webs using spacers. This approach could substantially reduce half-wave buckling under compression, improving the axial strengths of these columns, and enhancing overall stability. To date, research on such systems has been limited [26] below. Recent studies on these types of built-up columns have not yielded an easy and reliable design procedure [26]. The iterative nature of adopting Johnston's equation [32], accounting for the gap between chord members as suggested by Roy et al.[26], is cumbersome. The global slenderness calculation by Anbarasu and Dar (2020), based on AS/NZS 4600, overlooks the gap between columns, potentially misrepresenting the true behaviour of gapped channel sections. Moreover, the design equation by Rondal and Niazi [28][29] neglects the torsional effects on chord members due to the C-stitch geometry. Since stitches connect to the chord members' web through flanges, they offer unequal stiffness to panels above and below, increasing torsional buckling risk. Notably, the absence of torsional buckling in tests by Roy

et al. [26] was primarily due to the boundary conditions simulating pin-ended supports with a uniaxial hinge, which prevents torsion due to its directional fixity.

However, existing research on such systems remains limited, and current design standards such as Australian and New Zealand Standards AS/NZS 4600:2018[33] often overlook the beneficial effects of spacing between members. This is the case regardless of whether the Effective Width Method (EWM) or the Direct Strength Method (DSM) is used. It should be noted that the DSM does not include post-local-buckling capacity, however, Kumar and Kalyanaraman[35], modified the DSM equations, referred to here as M-DSM, to include post-local-buckling capacity. The axial strength calculated in accordance with the design standard has been presented in this study.

Due to inconsistencies and insufficient investigation into the spacing between channel sections and the number of required spacers, which are critical for cost savings, past research on these types of built-up columns is lacking. Therefore, it is necessary to explore the behaviour of such built-up systems in detail to enhance their structural performance. Based on the validated FE models, an extensive parametric study was conducted to investigate the axial compression capacity of CFS back-to-back gapped channel sections (Figure 1-2). Further, a comparison of the FEA prediction with AS/NZS has been carried out.

In this study, validated finite element models were used to conduct a comprehensive parametric investigation into the axial compression capacity of back-to-back gapped built-up CFS channel sections (see Figure 1-2). Additionally, comparisons were made between finite element analysis predictions and the strengths calculated in accordance with AS/NZS 4600:2018, highlighting discrepancies and opportunities for improving the design rules of AS/NZS 4600:2018.

CHAPTER 2. Literature review

2.1 Introductory remarks

This chapter presents an extensive literature review on the behavior of CFS channel sections with plain webs, under axial compression loading conditions. The literature review comprises two primary components. No research has been found in the literature investigating the effect of spacers on the axial capacity of back-to-back gaped channel sections.

2.2 Research on the CFS channel sections

This chapter presents an extensive literature review on the behavior of CFS single channel sections with plain webs under axial compression loading conditions. The literature review comprises two primary components. No research has been found in the literature investigating the effect of spacers on the axial capacity of back-to-back gaped channel sections.

The literature review on the cold-formed steel-lipped channel section columns undergoing local-overall buckling interaction provides a comprehensive overview of key studies conducted by various researchers. The study conducted by Roy et al.[50] mainly focuses on local-overall buckling interaction behavior of axially loaded cold-formed steel (CFS) channel section columns. A total of 40 tests were conducted on CFS channel sections covering stub, short, intermediate, and slender columns with varying thicknesses and a parametric study comprising 70 FE models was reported. The experimental and FE results are compared against the strength predictions in accordance with AISI (2016), AS/NZS (2018) and Eurocode (EN 1993-1-3). It was found that the AISI (2016) and AS/NZS (2018) are conservative by 10 to 15% on average when determining the axial capacity of pin-ended CFS channel section columns undergoing local-overall buckling interaction. Eurocode (EN 1993-1-3) design rules were found to lead to considerably more conservative predictions of column axial load capacity for CFS channels. This paper presents an experimental and finite element (FE) investigation into the local-overall buckling interaction behavior of axially loaded cold-formed steel (CFS) channel section

columns (Figure 2-1). Current design guidelines from the American Iron and Steel Institute (AISI) and the Australian and New Zealand Standards (AS/NZS) recommend the use of a non-dimensional strength curve for determining the axial capacity of such CFS channel section columns and therefore proposed modifications to the current design rules of AISI (2016) and AS/NZS (2018). The accuracy of the proposed design rules was verified using the FE analysis and test results of CFS channel section columns undergoing local-overall buckling interaction.

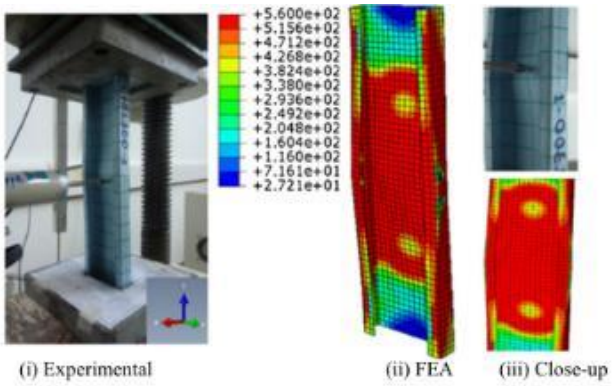

(a) Stub column (C75L300-1)

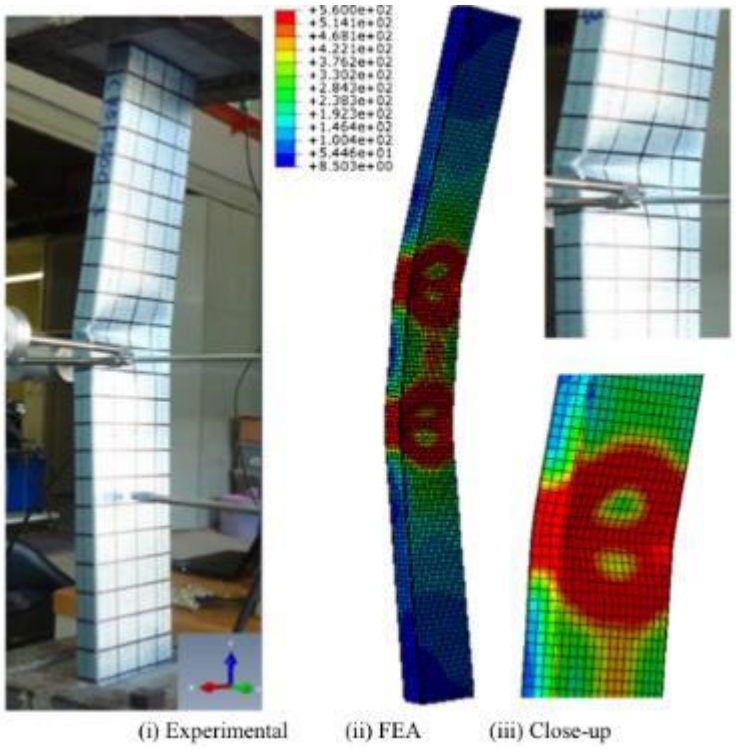

(b) Short column (C90L500-1)

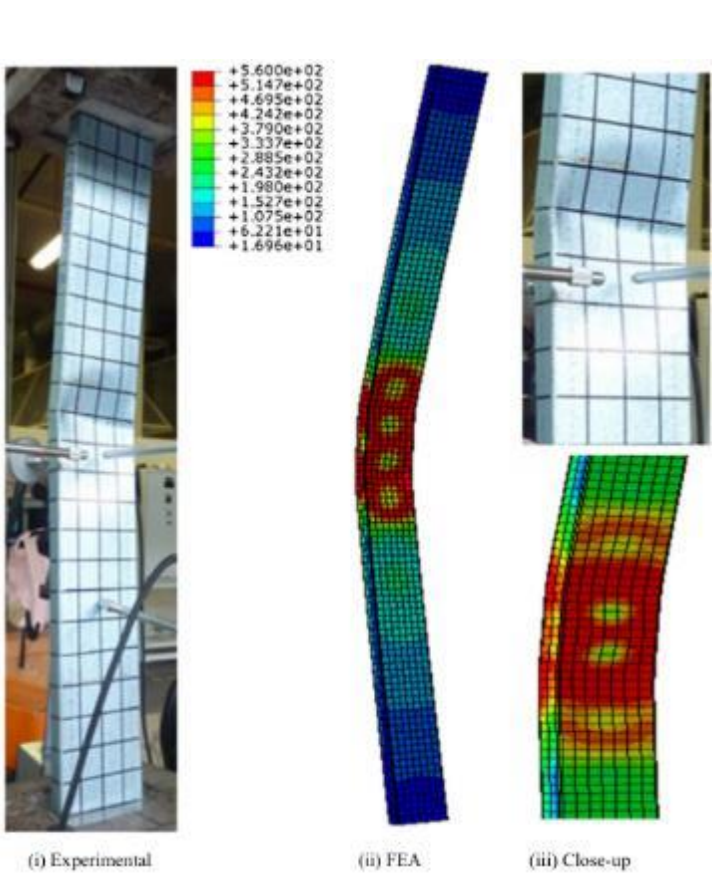

(c) Intermediate column (C75L1000-1)

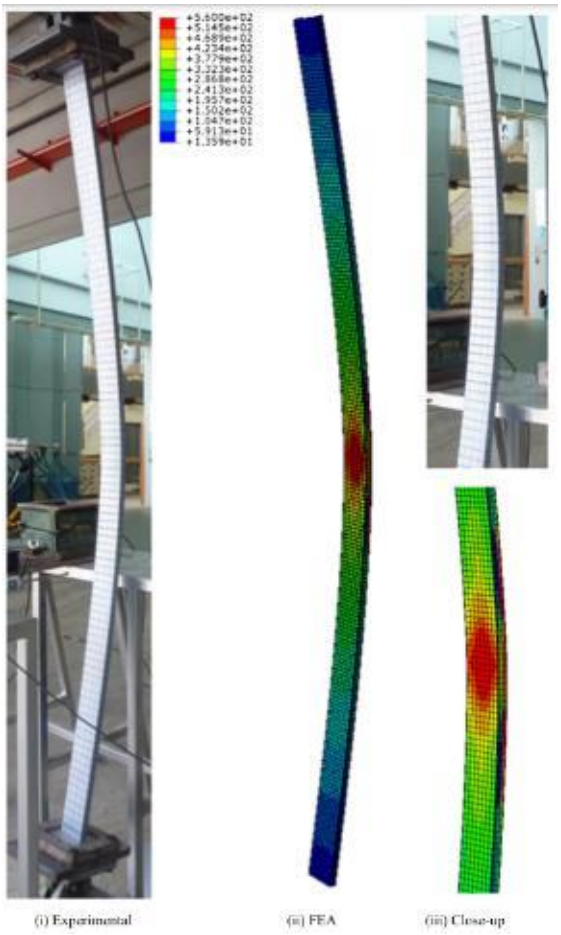

(d) Slender column (C75L2000-1)

Figure 2-1*:* Experimental Tests by Roy et al.[50] local-overall buckling interaction behaviour of axially loaded cold-formed steel (CFS) channel section columns and FE results comparison.

The investigation conducted by Dinis et al.[51] on the behavior of cold-formed steel (CFS) columns, specifically focused on the interaction between major-axis flexural-torsional (G-1) and minor-axis flexural (G-2) buckling modes, termed as global-global (G-G) interaction. The study aims to evaluate how well the Direct Strength Method (DSM) predicts the ultimate strength of CFS columns that exhibit G-G interaction under different conditions of length and end supports. The investigation study focuses mainly on Buckling Behavior: Studying the column buckling behavior is crucial for identifying geometries prone to G-G interaction, and Non-linear Behavior: Special attention is given to post-buckling behavior, particularly in identifying the most detrimental initial geometric imperfections. Based on gathered failure load

data across various yield stresses, modifications to the DSM-based design approach are proposed. These modifications aim to improve prediction accuracy for columns experiencing G-G interaction, specifically adjusting the load-to-buckling load ratio.

The investigation conducted by B. Boshra et al.[52] on the optimization of Cold-Formed Steel Channel Columns with Stiffeners. CFS columns under axial compression exhibit complex behavior influenced by geometric parameters and stiffener configurations. Key characteristics studied include ultimate load capacity, stiffness, ductility and energy absorption. To optimize the performance of CFS channel columns with stiffeners, advanced methodologies such as the Taguchi method coupled with grey relational analysis have been applied. In conclusion, optimizing CFS channel columns with stiffeners involves a comprehensive understanding of their behavior characteristics and the application of advanced optimization techniques. The integration of the Taguchi method with grey relational analysis provides a robust framework for designing columns that meet performance requirements across multiple criteria.

The study conducted by Gustavo Y. Matsubara et al. on Lipped channel cold-formed steel columns under local-distortional buckling mode interaction. This study focuses on the structural behaviour and design optimization of lipped channel cold-formed steel (CFS) columns under local-distortional (LD) buckling interaction. Using experimental data to calibrate a shell finite element model, the research examines a wide range of distortional-local slenderness ratios to simulate various LD buckling conditions accurately. Key parameters such as the local slenderness factor (λL), distortional slenderness factor (λD), and the distortional-local slenderness ratio ($R\lambda DL = \lambda D / \lambda L$) are analysed to understand their impact on column strength variation. The study establishes a Winter-type equation within the framework of the direct strength method (DSM), providing a practical and accurate tool for predicting column strength under LD interaction scenarios. This approach aims to streamline structural design

processes for lipped CFS columns, ensuring robustness and efficiency in engineering applications.

2.3 Summary of CFS channel sections literature review

Roy et al.[50] highlight the discrepancy between current design codes and actual behavior observed in experiments and FE analysis of CFS channel section columns undergoing local-overall buckling interaction. Their proposed modifications aim to enhance the accuracy of axial capacity predictions in design guidelines.

The study of Dinis et al.[51] addresses the complex interaction between major and minor axis buckling modes in CFS columns, emphasizing the need for improved predictive methods under diverse structural conditions. Their proposed modifications to the DSM aim to better align design predictions with observed behavior in columns prone to G-G interaction.

Boshra et al.[52] study contributes to optimizing the design of CFS channel columns with stiffeners by leveraging advanced optimization methodologies. Their approach enhances the structural performance of CFS columns under axial compression, addressing complex behaviors influenced by geometric variations and stiffener configurations.

Matsubara et al. study provides a comprehensive framework for understanding and predicting the behavior of lipped channel CFS columns under local-distortional buckling interaction. Their integration of experimental data with finite element modelling and the development of a tailored strength prediction equation contributes significantly to advancing the design methodologies for such structural elements.

2.4 Research on the CFS built-up channel section

This chapter presents an extensive literature review on the behavior of CFS back-to-back and face-to-face channel sections with, and plain web under axial compression loading conditions. The literature review comprises two primary components. No research has been found in the literature investigating the effect of spacers on the axial capacity of back-to-back gaped channel sections.

Anbarasu et al.[53] on axial capacity of CFS built-up columns comprising of lipped channels with spacers: Nonlinear response and design, presents a numerical investigation focused on pin-ended cold-formed steel (CFS) built-up columns constructed using back-to-back lipped channel sections connected by spacers. The study aims to assess the axial capacity and nonlinear deformation response under monotonic axial loading conditions. Finite element (FE) models were developed and validated against experimental data from similar configurations (Figure 2-2). A comprehensive parametric study varied parameters such as plate slenderness of the lipped channels, unbraced chord slenderness, and global slenderness to analyze their impact on the ultimate compression resistance of these columns. The effective width method, as per AS/NZ and European specifications for cold-formed steel structures, was initially used but revealed shortcomings in predicting strengths for built-up columns with spacers. Consequently, new design equations were proposed to enhance the accuracy of strength predictions for these configurations. The incorporation of spacers was found to reduce the local buckling half-wavelength, significantly improving the columns' buckling resistance, particularly in cases where failure was dominated by local buckling modes.

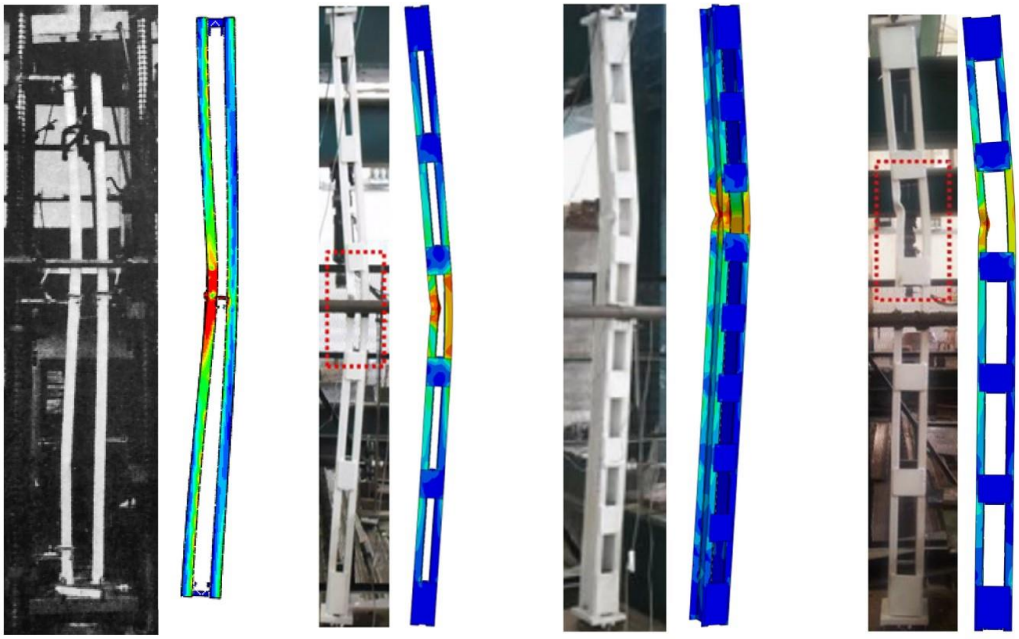

(a)

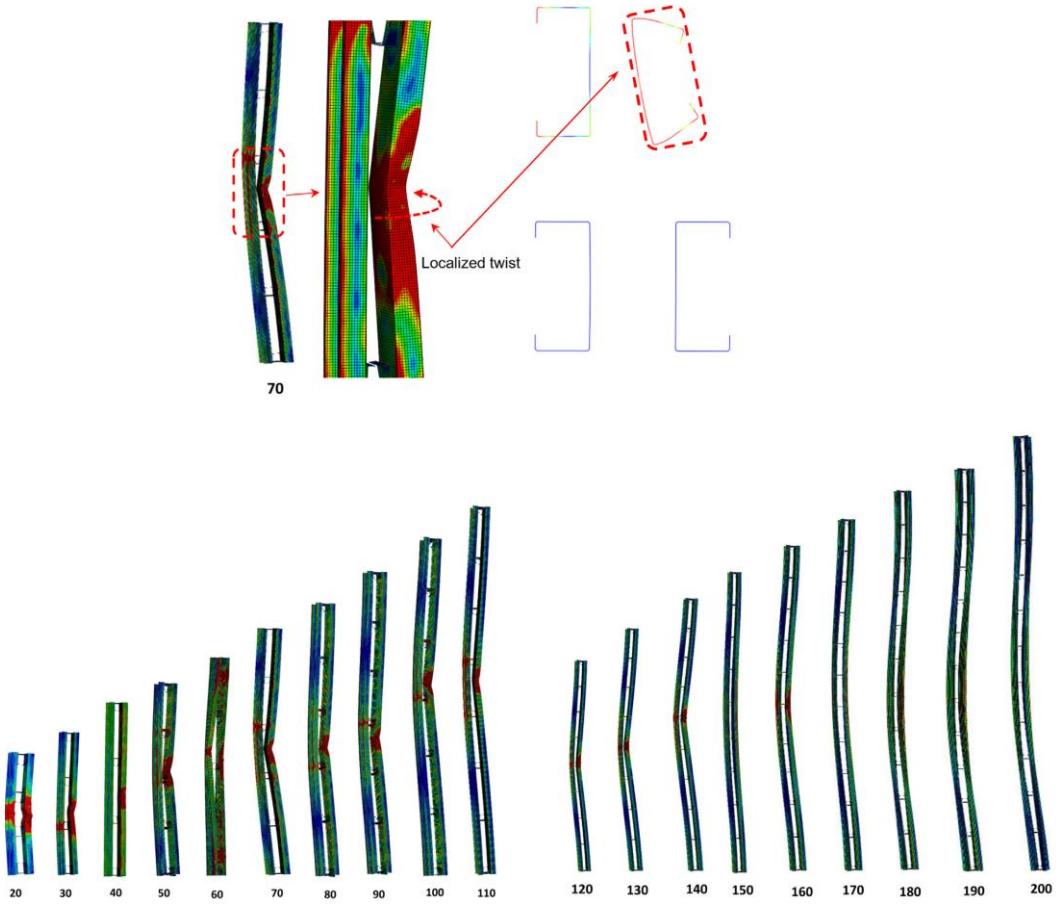

(b)

Figure 2-2: Experimental setup used by Anbarasu et al.[53] (a) Comparison of failure modes from the test and FE modelling, (b) Non-linear FE analysis deformed shapes for 120 × 50 × 15–1.2 Series.

Roy et al.[54] address the lack of comprehensive research in this area by conducting experimental tests on both configurations. For face-to-face sections, 36 tests cover a wide slenderness range, validating results with a nonlinear finite element model (Figure 2-3) that incorporates material non-linearity, imperfections, and fastener modelling. Results show that design standards (AISI, AS/NZS, Eurocode) are generally conservative by around 15%, but can underestimate local buckling failures by 8% on average. Similarly, back-to-back sections are investigated through 40 tests across various slenderness ratios, revealing that design standards can be overly conservative by up to 53%. Adjustments considering the gap between sections reduce conservatism to within 5% of experimental and FE results. These findings underscore the need for refined design approaches tailored to these configurations to optimize structural efficiency and reliability in cold-formed steel construction.

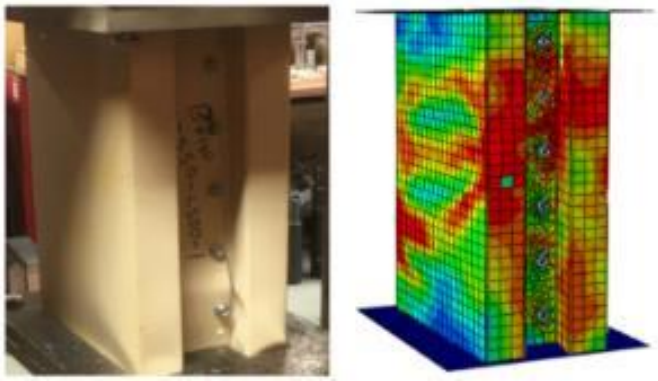

(a)

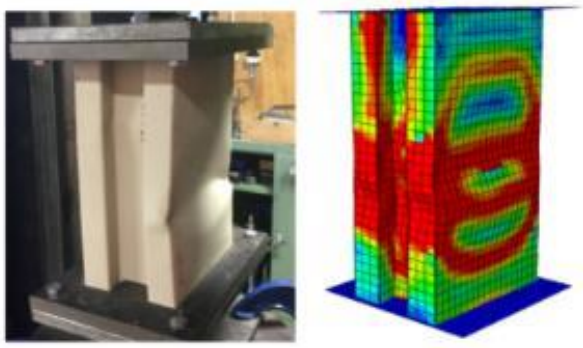

(b)

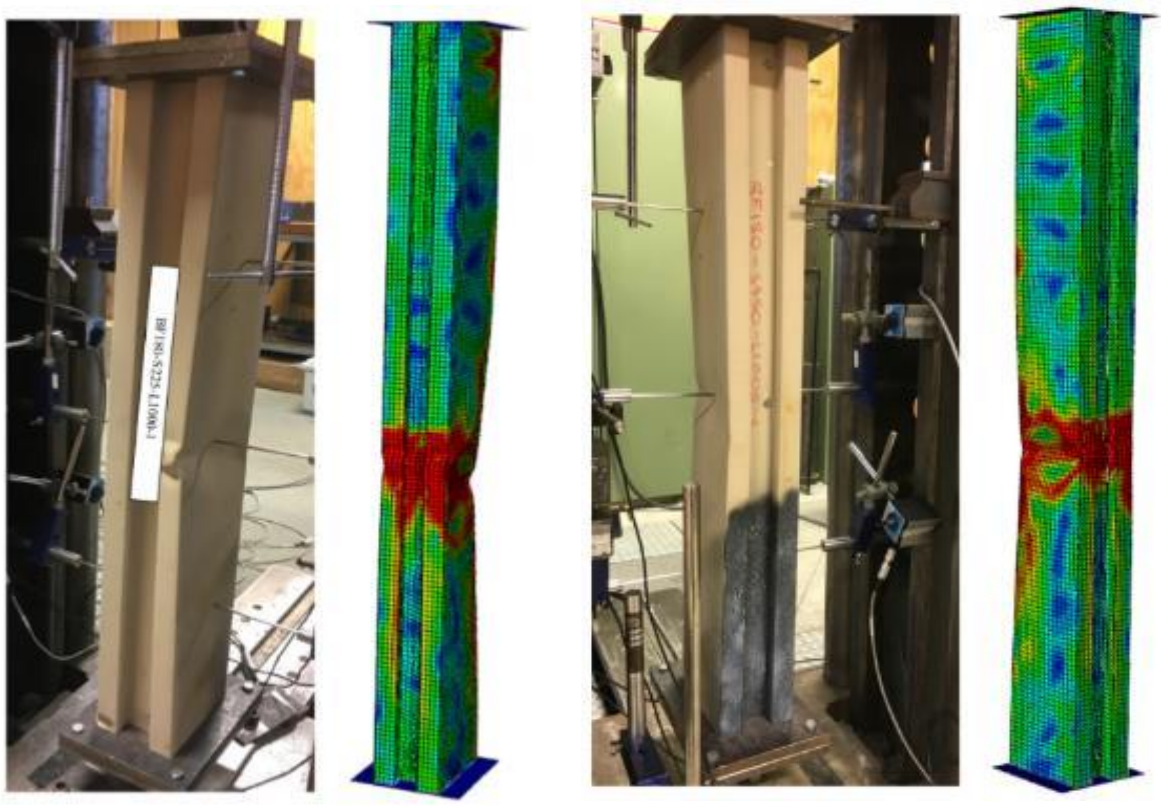

(c) (d)

Figure 2-3: Experimental setup used by Roy et al[54] Deformed shapes at failure face-to-face built-up cold-formed steel channel sections. Stub columns: (a) BF180-S50-L300, (b) BF180-S100-L300, Intermediate columns: (c) BF180-S225-L1000, (d) BF180-S450-L1000

Roy et al [26] investigate the nonlinear behavior of axially loaded back-to-back built-up cold-formed steel un-lipped channel sections, which are commonly utilized in structures like trusses, wall frames, and portal frames. Unlike lipped channel sections, there is a lack of experimental tests and finite element analyses specifically addressing this configuration and the impact of screw spacing on axial strength. The study presents results from 95 finite element analyses covering a range from stub to slender columns. The finite element model is validated against recent experimental tests on back-to-back built-up cold-formed steel-lipped channel sections. A parametric study using the validated model explores the effect of screw spacing on axial strength, revealing that un-lipped sections exhibit approximately 31% lower axial strength on average compared to lipped channel sections. Furthermore, design standards such as the

American Iron and Steel Institute (AISI) and Australian and New Zealand Standards (AS/NZS) are found to be overly conservative by around 15% for columns failing through overall buckling, while underestimating strengths by approximately 8% for columns primarily failing through local buckling. These findings underscore the need for tailored design guidelines to optimize the performance and efficiency of back-to-back built-up cold-formed steel un-lipped channel sections in structural applications.

Roy et al.[13] investigate the effect of thickness on the behavior of axially loaded back-to-back built-up cold-formed steel channel sections, increasingly utilized in structures like trusses, wall frames, and portal frames. The study addresses the lack of comprehensive research on how column thickness and slenderness affect axial capacity in such configurations. Sixty experimental tests were conducted under compression, varying column thickness, length, and cross-section to observe different failure modes and strengths. A nonlinear finite element model was developed and validated against experimental data (Figure 2-4), incorporating material non-linearity, geometric imperfections, and explicit modelling of web fasteners. A parametric study with 204 models explored a wide range of thicknesses and slenderness ratios. Results highlighted discrepancies with current AISI & AS/NZS standards, showing these standards to be overly conservative for intermediate and slender columns prone to overall member buckling, yet un-conservative for stub and short columns failing primarily through local buckling. The study proposes improved design rules based on these findings, validated through rigorous comparisons with experimental and numerical results. This approach aims to enhance the accuracy and reliability of design guidelines for back-to-back built-up cold-formed steel channel sections subjected to axial compression.

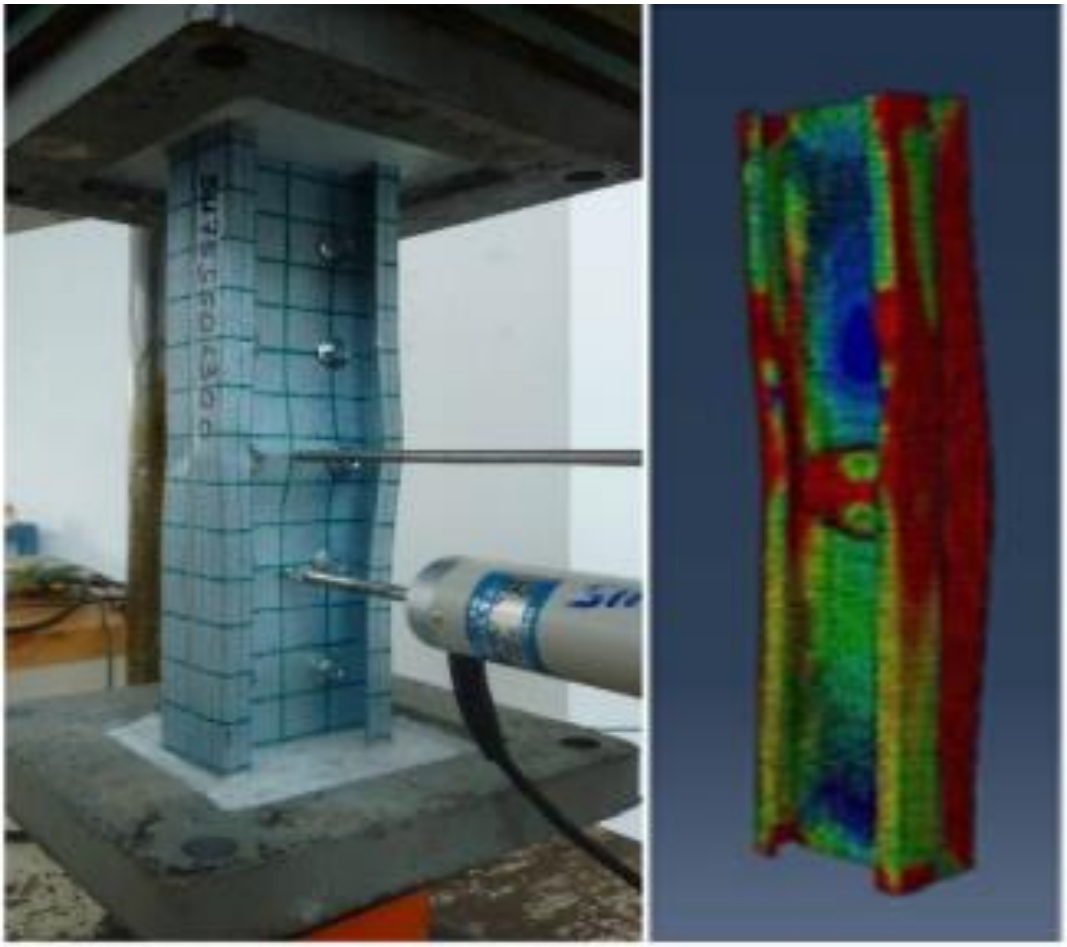

(a)

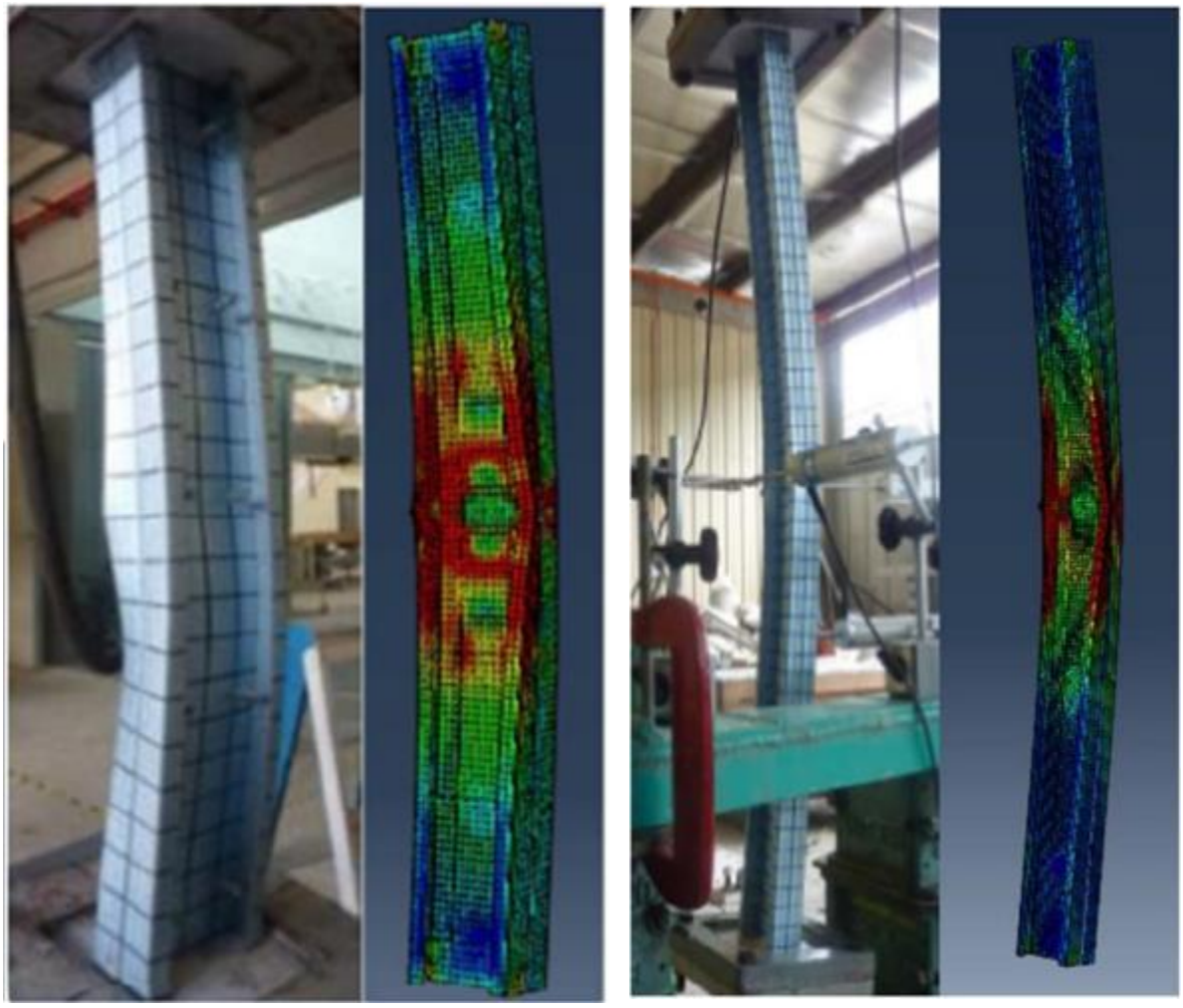

(b) (c)

Figure 2-4: Experimental setup used by Roy et al.[13] Failure modes of built-up sections. (a) Stub column, (b)Short column, (c)Intermediate column.

The study conducted by Roy et al.[55] investigates the influence of screw spacing on the behavior of axially loaded back-to-back built-up cold-formed steel channel sections, increasingly used in cold-formed steel structures such as trusses, wall frames, and portal frames. The research addresses the gap in understanding by conducting 30 experimental tests across a range of column types from stub to slender. These tests provide insights into how screw spacing affects column behavior. A finite element model, validated against experimental results, further explores this relationship through a parametric study comprising 144 models. The study reveals that while the modified slenderness approach recommended by standards

like AISI and AS/NZS is generally conservative, it can underestimate the strength of stub columns by approximately 10%. This finding underscores the need for nuanced design considerations when applying standards to back-to-back built-up cold-formed steel channel sections, particularly concerning the spacing of intermediate fasteners to optimize structural performance and reliability in practical applications.

Roy et al.[56] presents a finite element modelling study focused on back-to-back built-up cold-formed steel (CFS) un-lipped channel sections under axial compression, a configuration increasingly used in structures like trusses and portal frames. The finite element model, developed using ABAQUS, incorporates material non-linearity, initial imperfections, and explicit modelling of intermediate web fasteners to simulate realistic behavior. Validation of the model against experimental results from previous studies ensures its accuracy. A parametric study using the validated model investigates the influence of screw spacing on axial strength across various column configurations. Results indicate discrepancies with current AISI & AS/NZS design standards: while these standards prove overly conservative for columns failing due to overall buckling, they are found to be un-conservative for stub and short columns prone to local buckling. This research underscores the need for refined design approaches that account for specific configurations and loading conditions to optimize the structural efficiency and reliability of back-to-back built-up CFS un-lipped channel sections in practical applications.

Analysis to determine flexural buckling of cold-formed steel built-up back-to-back section columns (Figure 2-5) presented by Tianhua Zhou et al.[14] introduces a novel analytical approach to determine the flexural buckling capacity of cold-formed steel (CFS) built-up back-to-back section columns, challenging the conventional Modified Slenderness Method (MSM) used in current AISI standards. The study proposes a new flexural buckling model that establishes kinematic relationships for individual profiles within the built-up column. It

incorporates shear panels at screw locations to account for discrete shear deformation restraints, determining shear rigidity through cross-sectional shear stress transfer paths. Using the energy method, the study derives a computation method that is then simplified for practical engineering applications. Validation of the derived formula is conducted through a finite element model (FEM), which is calibrated and verified against experimental data. Parametric studies using the FEM further validate the formula's predictions. Comparative analysis with direct strength method (DSM) expressions based on test results confirms that the derived formula accurately predicts critical flexural buckling loads and strengths. It also highlights that increasing screw spacing can lead to significantly conservative estimates using the MSM for CFS built-up back-to-back section columns. This research underscores the importance of refined analytical methods to optimize design and enhance structural efficiency in CFS construction.

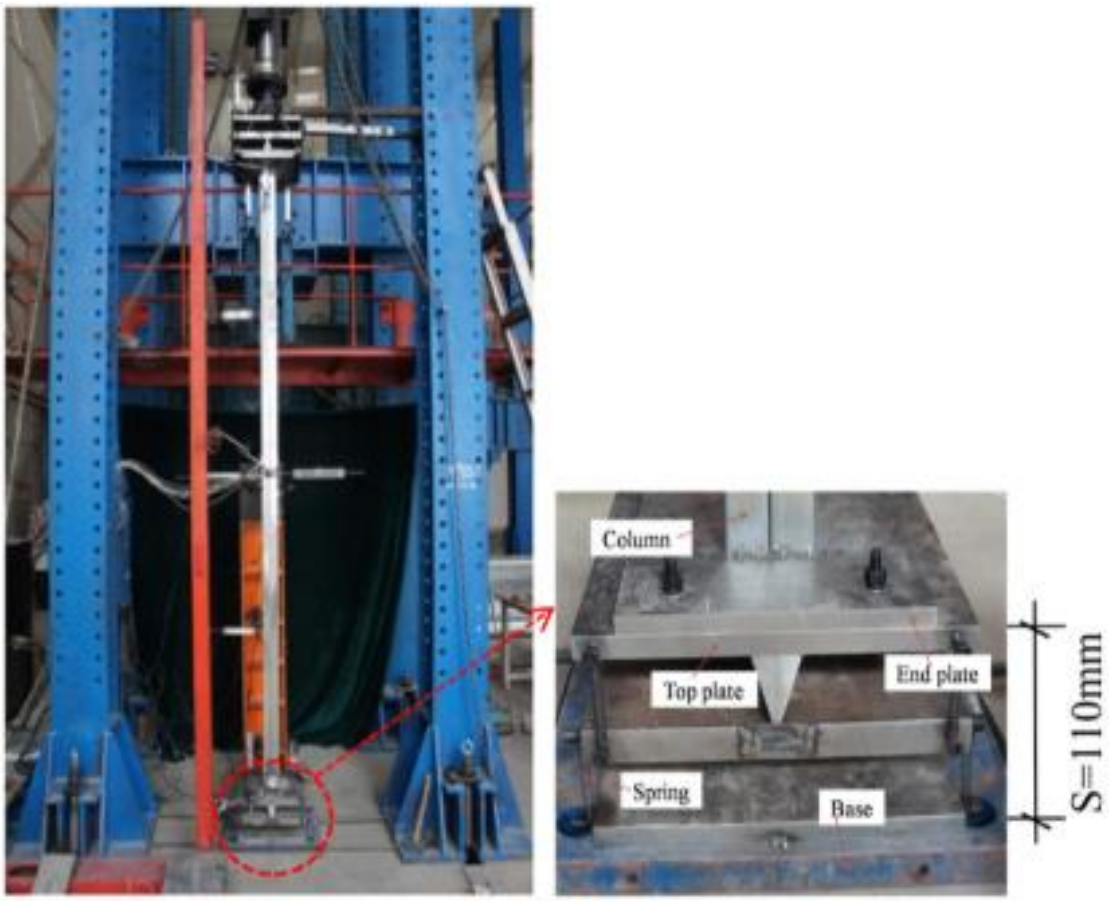

Figure 2-5: Experimental setup used by Tianhua Zhou et al.[14] for non-linear static analysis

An investigation study by Tianhua Zhou et al.[57] focuses mainly on investigating the elastic buckling behavior of composite webs in cold-formed steel (CFS) back-to-back built-up columns through a combination of experimental tests and finite element (FE) analyses. Eighteen CFS back-to-back built-up columns were tested, each constructed from two identical C-section components joined with self-drilling screws at their webs. The research explores the influence of screw number and spacing on critical buckling loads and modes of these built-up columns. Parametric studies using FE models, validated against experimental results, further investigated these effects in detail. The FE analyses successfully predicted both critical buckling loads and buckling modes, demonstrating good agreement with laboratory test observations. This comprehensive approach provides valuable insights into optimizing the design and performance of CFS back-to-back built-up columns in structural applications, highlighting the benefits of integrating experimental and numerical methods for accurate structural assessment and design refinement.

A study by AM Mahar et al.[58] addresses inconsistencies in the design approach for built-up cold-formed steel (CFS) columns outlined in Section I1.2 of the AISI S100 specification. By integrating findings from a compound spline finite strip-based numerical framework and analyzing 228 experimental and numerical results from existing literature, the study proposes a refined design equation. Numerical models incorporating mode-specific deformations within the framework assessed the shear slip behavior influenced by factors like fastener spacing and slenderness ratio of fully composite cross-sections through parametric variations. The research highlights that the Modified Slenderness Ratio (MSR) in AISI S100 tends to provide overly conservative strength predictions with increased fastener spacing, as it treats the effects of fastener spacing and overall slenderness ratio as separate and additive. To better reflect their interactive nature, a Compound Slenderness Ratio (CSR) is introduced, which accounts for this interaction more accurately. The proposed CSR, integrated with the Direct Strength Method

(DSM), demonstrates close alignment between predicted and observed strengths from experimental and numerical studies. This approach enhances the reliability of DSM design equations and offers a refined framework for optimizing the design of built-up CFS columns in structural applications.

An investigation study by AR Dar et al.[59] investigates wide-flanged cold-formed steel (CFS) built-up columns using edge-stiffened channels aligned back-to-back, aiming to explore their structural performance compared to traditional narrow-flanged CFS channels. The research is structured into three main components. First, fourteen specimens under warping restrained pinned end conditions undergo comprehensive testing, covering material properties, geometric imperfections, compressional resistance, load-axial shortening behavior, and deformation characteristics. The second component involves developing a nonlinear finite element model that incorporates material and geometric nonlinearity to validate the experimental findings. Results from both tests and numerical simulations demonstrate good agreement in terms of ultimate compressional resistance, load-axial shortening curves, and deformed shapes. The third component focuses on quantifying design strengths using the Direct Strength Method (DSM) and Effective Width Method, comparing these against the experimental strengths. The study reveals a conservative trend in strength predictions and examines the reliability of design rules. It identifies a degradation in axial strength and stiffness with increasing column slenderness, attributing failure modes to interactive buckling involving local and distortional buckling, distortional and flexural buckling, and local and flexural buckling. Overall, this research provides valuable insights into optimizing the design and performance of wide-flanged CFS built-up columns in structural applications, addressing gaps in the existing literature and enhancing understanding of their behavior under axial compression.

2.5 Summary of CFS built-up channel sections literature review

Anbarasu et al.[53] investigated the axial capacity and nonlinear deformation of pin-ended cold-formed steel (CFS) built-up columns with back-to-back lipped channels and spacers. Validated finite element models showed that varying plate, unbraced chord, and global slenderness affected compression resistance. Existing design methods (AS/NZ, European) were inadequate, leading to new design equations. Spacers reduced local buckling half-wavelength, significantly improving buckling resistance, especially in columns prone to local buckling.

Roy et al.[54] conducted tests on cold-formed steel (CFS) built-up columns in face-to-face and back-to-back configurations. For face-to-face sections, 36 tests showed design standards (AISI, AS/NZS, Eurocode) were generally conservative by 15% but underestimated local buckling by 8%. For back-to-back sections, 40 tests revealed standards were overly conservative by up to 53%. Adjusting for the gap between sections reduced this conservatism to 5%. The study calls for refined design approaches to enhance structural efficiency and reliability in CFS construction.

Roy et al.[26] studied the nonlinear behavior of axially loaded back-to-back built-up cold-formed steel (CFS) un-lipped channel sections. Through 95 finite element analyses and validation against experimental tests, they found un-lipped sections to have 31% lower axial strength than lipped sections. Current design standards (AISI, AS/NZS) were overly conservative by 15% for overall buckling and underestimated local buckling strengths by 8%. The study suggests the need for refined design guidelines for these CFS sections.

Roy et al.[54] investigated the effect of thickness on axially loaded back-to-back built-up cold-formed steel (CFS) channel sections. Sixty experimental tests and a validated nonlinear finite element model were used to study variations in column thickness, length, and cross-section. A parametric study with 204 models showed that current AISI and AS/NZS standards are overly

conservative for intermediate and slender columns prone to overall buckling, but under-conservative for stub and short columns failing through local buckling. The study proposed improved design rules to enhance the accuracy and reliability of design guidelines for these CFS sections.

Tianhua Zhou et al.[14] proposed a new model for determining the flexural buckling capacity of cold-formed steel (CFS) built-up back-to-back columns, challenging the current Modified Slenderness Method (MSM). The model includes kinematic relationships and shear restraints, validated through finite element models and experimental data. It accurately predicts buckling loads and shows that increasing screw spacing leads to conservative MSM estimates. The study emphasizes refined analytical methods to improve CFS design efficiency.

Tianhua Zhou et al.[57] investigated the elastic buckling behavior of composite webs in cold-formed steel (CFS) back-to-back built-up columns. They conducted experimental tests on 18 columns joined with self-drilling screws, analyzing the impact of screw number and spacing on critical buckling loads and modes. Parametric studies using finite element models validated against experiments confirmed the accuracy of predictions for buckling loads and modes. The study underscores the importance of integrating experimental and numerical methods to optimize the design and performance of CFS back-to-back built-up columns in structural applications.

AM Mahar et al.[58] addressed inconsistencies in AISI S100 for built-up cold-formed steel (CFS) columns by proposing a refined design equation. Their study integrated findings from a compound spline finite strip-based numerical framework and analyzed 228 experimental and numerical results. They introduced a Compound Slenderness Ratio (CSR) to better account for the interactive effects of fastener spacing and slenderness ratio, which the Modified Slenderness Ratio (MSR) in AISI S100 tends to overestimate. The CSR, integrated with the

Direct Strength Method (DSM), improved strength predictions and enhanced the reliability of design equations for optimizing built-up CFS column designs.

AR Dar et al.[59] studied wide-flanged cold-formed steel (CFS) built-up columns using back-to-back edge-stiffened channels. They conducted comprehensive experimental tests and validated results with a nonlinear finite element model. Findings showed good agreement in compressional resistance, load-axial shortening behavior, and deformation characteristics. The study highlighted conservative strength predictions and identified degradation in axial strength and stiffness with increased column slenderness, addressing gaps in understanding and optimizing the design of these columns in structural applications.

2.4 Research Problem/Gap Found in Literature Review

Given the inconsistencies and lack of thorough investigation into the spacing between channel sections and the required number of spacers, which are crucial for cost efficiency, past research on built-up columns has significant gaps. This underscores the necessity to explore the behaviour of such built-up systems in detail to enhance their structural performance.

Although extensive studies have been conducted on back-to-back gapped channel sections under axial compression and those with longitudinal spacings, there is a notable gap in the literature regarding the behaviour of these sections with spacers under axial compression. Specifically, while some research has investigated the use of spacers, the optimal number of spacers relative to the column length has not been determined. Moreover, the effect of transverse spacing on the axial capacity of these sections remains unaddressed. This oversight highlights the critical need for more comprehensive studies to fully understand and optimize the structural performance of back-to-back gapped channel sections with spacers, addressing both the optimal number and arrangement of spacers for improved stability and strength.

2.6 Aim and scope of this research.

The objective of this thesis is to investigate the axial capacity of CFS back-to-back gapped channel sections with a minimum number of equally spaced spacers subjected to compression. The investigation will be performed based on the finite element analysis. Specific objectives of this work are listed below:

To establish nonlinear finite-element (FE) models to simulate the structural behavior of CFS channel sections subjected to compression. The measured cross-section dimensions, material properties obtained from the literature and geometric imperfections were also included in the FE models. The FE models will then be validated against the results obtained from the tests conducted by Roy et al.[26] in terms of deformed shapes, and axial capacity.

The validated FE models will be used to perform a parametric study involving 1000 FE models to investigate the influence of different parameters on the capacity of such CFS back-to-back gapped channel sections with a minimum number of equally spaced spacers subjected to compression.

To evaluate the performance of current design guidelines while predicting the capacity of CFS back-to-back gapped channel sections with a minimum number of equally spaced spacers, FEA results will be compared against the design strengths predicted by the current design guidelines, AS/NZS-4600:2018.

Based on the results obtained from the parametric study, suitable conclusions will be summarized for calculating the axial capacity of CFS back-to-back gapped channel sections with a minimum number of equally spaced spacers.

2.7 Outline of the thesis

This thesis is focused on the axial capacity of CFS back-to-back gapped channel sections with a minimum number of equally spaced spacers subjected to compression. The thesis is structured into the following six chapters:

Chapter 1 Briefly introduces the background, problem statement, and outline of the thesis.

Chapter 2 Summarizes the literature review on the behavior and design of CFS single, back-to-back with no gap and back-to-back gapped channel sections with plain webs subjected to axial compression.

Chapter 3 Describes the summary of experimental studies.

Chapter 4 Describes the development of Finite Element Analysis, a new methodology application in FE analysis, numerical investigation and validation of back-to-back gapped channel sections to assess the axial capacity.

Chapter 5 Provides Parametric comparison with the design study and current design rule Australia and New Zealand Standard (AZ/NZS) [33].

Chapter 6 Provides conclusions including the limitations of the current study and recommendations for future researchers and practicing engineers.

CHAPTER 3. Summary of Experimental Studies

3.1 General

In this chapter, the results of experimental tests are presented by Roy et al. [26] on back-to-back gapped built-up cold-formed steel channel sections, with the sections acting as columns, are considered for validation (**Error! Reference source not found.**-1). The experimental tests reported by Roy et al. (2018) had a value of non-dimensional slenderness ranging from 0.23 to 1.42, thus covering stub to slender columns.

Table 4-1 summarises the measured column dimensions along with compressive strength obtained through experimental testing. The experimental test program comprised 40 specimens, subdivided into four different column heights: 300 mm, 500 mm, 1000 mm, and 2000 mm. All columns with pin-ended, other than the 300mm columns which were tested as fixed-ended columns.

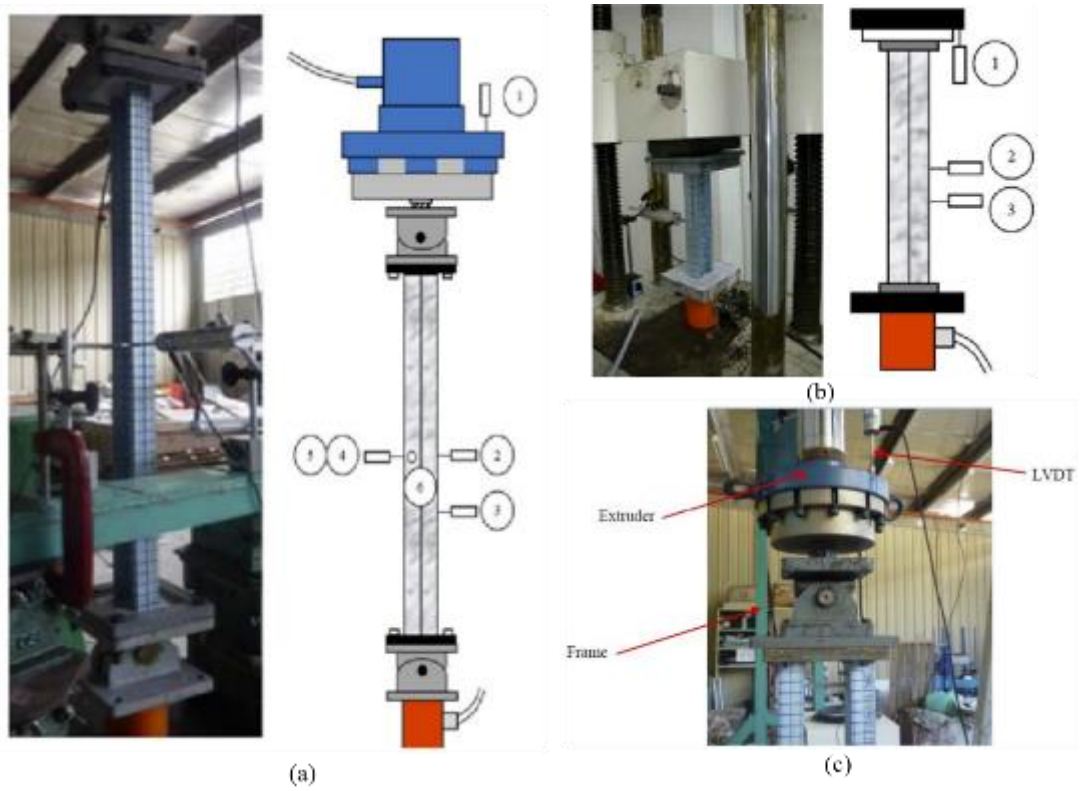

Figure 3-1: Details of the test carried out by Roy et al. (2018), (a) Slender column, (b) stub column, (c) Support condition and position of LVDT for measuring shortening

CHAPTER 4. Development of Finite Element Analysis

4.1 General

Previous research has demonstrated that finite element (FE) analysis using ABAQUS and ANSYS software is both efficient and reliable for predicting the structural performance of thin-walled cold-formed steel (CFS) elements and connections under a variety of loading conditions. These tools have proven capable of accurately simulating the behavior of CFS structures, which are often characterized by their lightweight and high strength-to-weight ratio. Using ABAQUS and ANSYS, can model complex geometries and material properties, apply various load scenarios, and analyze the resulting stress distributions, deformations, and potential failure modes. This capability is crucial for designing and optimizing CFS structures, ensuring they meet safety and performance standards. The detailed insights gained from such analyses help in refining design parameters, improving connection details, and enhancing the overall structural integrity and efficiency of CFS elements used in construction. Consequently, these software platforms have become indispensable in the field of structural engineering for the analysis and design of thin-walled CFS components.

In the current study, the comparison of experimental values with compressive strengths predicted by Roy et al. [26] on the comparison of experimental values with compressive strengths predicted by the finite element analysis was used to validate the developed FE model.

4.2 New methodology application in FE analysis

The current study introduces a new methodology in finite element (FE) analysis to enhance the accuracy and reliability of predicting the structural performance of thin-walled cold-formed steel (CFS) elements. This innovative approach builds upon the established use of ABAQUS and ANSYS software, incorporating several advanced techniques to refine the modelling process.

Precise Modeling of Imperfections: The new methodology involves a more detailed representation of initial geometrical imperfections in CFS elements, which are critical in capturing the actual behavior of the structure under load. This includes utilizing high-resolution scanning methods to incorporate real-world imperfections into the FE model.

Complex Geometry Handling: The approach allows for the accurate modelling of complex geometrical features and connections, which are often simplified in conventional methods.

Nonlinear Material Properties: Incorporating advanced material models that account for the nonlinear stress-strain behavior of CFS, including strain hardening and anisotropy, enhances the accuracy of predictions.

Accurate Boundary Conditions: Enhanced techniques for applying boundary conditions more accurately represent the constraints and supports present in actual structures.

Experimental Correlation: The methodology emphasizes extensive validation and calibration against experimental data. The comparison of experimental compressive strengths with predictions from Roy et al. [26] and the newly developed FE model ensures that the simulations closely match observed behaviors.

Iterative Refinement: Continuous refinement of the FE model based on experimental feedback helps in progressively improving the accuracy of predictions.

In summary, the new methodology in FE analysis represents a significant advancement in the modelling and simulation of thin-walled cold-formed steel structures. By addressing the limitations of previous approaches and incorporating state-of-the-art techniques, this methodology provides a more accurate, dependable, and insightful tool for structural engineers, ultimately contributing to the development of safer and more efficient CFS constructions.

Figures 4.1-4.4 illustrate the integration process of Ansys and Abaqus for finite element (FE) analysis modelling. This hybrid approach leverages the unique strengths of both software platforms to achieve a comprehensive analysis of structural behavior.

Figure 4.1 demonstrates the first step in the model creation process, where the geometry and boundary conditions are established using Ansys. This phase includes configuring the structural model, applying loads, setting material properties, and defining initial geometric imperfections.

Figure 4.2 illustrates the process of exporting the model from Ansys to Abaqus. This step involves converting the Ansys models into input (.inp) files that are compatible with Abaqus, facilitating the smooth transfer of geometry, mesh, and boundary conditions.

Figure 4.3 shows the next phase of the analysis within Abaqus, where the multiple input (.inp) files generated in the previous step are merged. At this stage, numerous FE models can be automatically executed in Abaqus by running a Windows batch file. This method optimizes the process of executing multiple FE models, thereby saving time and effort for engineers and analysts.

The batch file is scripted with commands to run each FE model one after the other, ensuring efficient and automated processing of simulation tasks. This automation not only streamlines the workflow but also reduces the potential for human error, enhances productivity, and ensures consistency in the execution of large-scale finite element analyses. By automating the execution sequence, engineers can focus on analyzing the results rather than managing the execution of each individual model, thus significantly improving overall efficiency.

Finally, Figure 4.4 depicts the post-processing and analysis of results obtained from Abaqus. In this stage, valuable insights into the structural response are extracted by visualizing various data sets, such as stress distributions, displacement patterns, and other relevant metrics.

This process involves using Abaqus' post-processing tools to interpret and evaluate the performance of the design. Detailed visual representations, such as contour plots and deformation animations, to better understand how the structure behaves under different loading conditions. Additionally, numerical data can be extracted for further analysis, enabling the

identification of critical stress points, potential failure zones, and areas that may require design modifications. This comprehensive evaluation helps in optimizing the design, ensuring safety, and enhancing performance. The insights gained from this analysis are crucial for making informed decisions and improving overall structural integrity and efficiency.

Overall, this combined use of Ansys and Abaqus not only improves the accuracy and efficiency of FE analysis but also ensures that engineering structures are designed with the highest levels of reliability and safety.

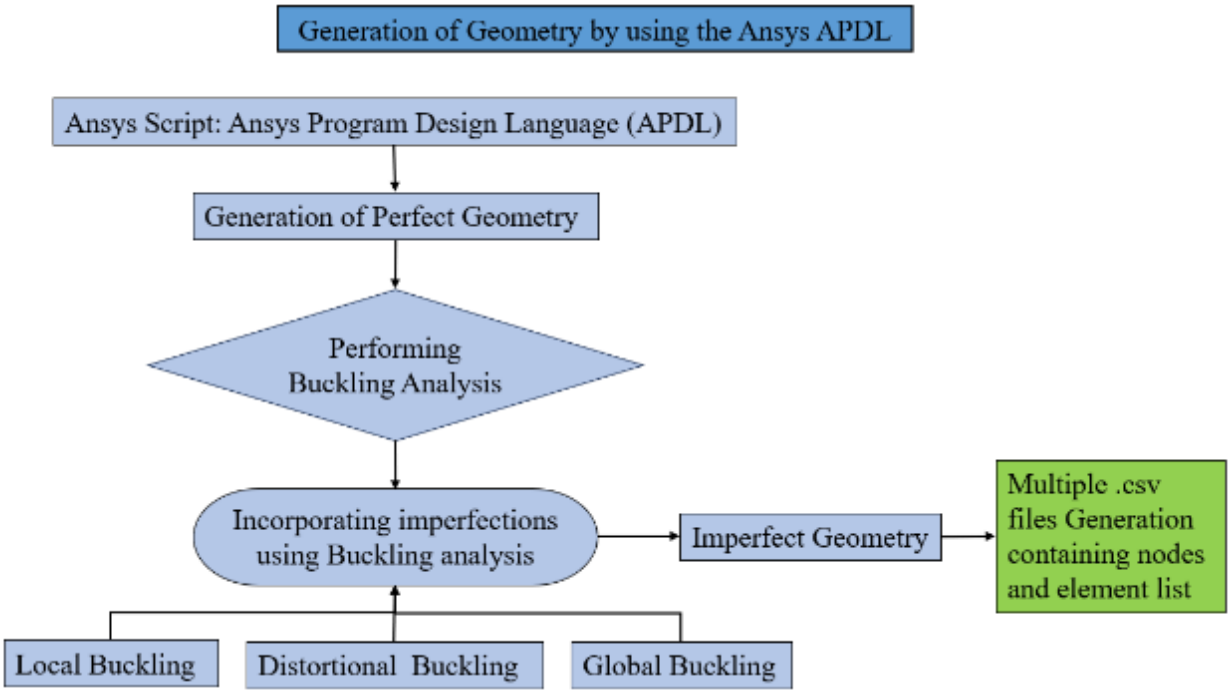

Figure 4-1: Imperfect geometry creation using Ansys APDL.

Figure 4-2: Creation of Abaqus input files.

Figure 4-3: FE Analysis execution using Abaqus Batch mode.

Figure 4-4: Post-processing of Data (.dat) files using Python.

4.3 Numerical investigation

4.3.1 General

ABAQUS [36] was used to develop a non-linear elastoplastic numerical model based on the measured centre-line dimensions of the cross-sections. Displacement-controlled loading was applied through the center of gravity of the specimens for the axial load. The numerical modelling incorporated geometric non-linearity and initial geometric imperfections. Relevant modelling details are described below.

4.3.2 Geometry and material properties

The complete geometry of the specimens was modelled based on the measured dimensions and material properties reported in the companion paper [28-30]. An elastic-perfect plastic material model obeying the Von Mises yield criterion was deemed adequate for considering the material properties [4][24][36] and was adopted accordingly. The yield stress of 565 MPa, along with Young's modulus of 205 GPa, was used in the numerical modelling of the parametric models.

According to the ABAQUS manual [36], the engineering stress-strain curve is converted into a true stress-strain curve using the following equation:

$$\sigma_{true} = \sigma(1 + \epsilon) \quad (1)$$

$$\epsilon_{true(pl)} = \ln(1 + \epsilon) - \frac{\sigma_{true}}{E} \quad (2)$$

where E is the Young's modulus, σ_{true} is the true stress, σ_u is the tensile ultimate strength, σ and ε are the engineering stress and strain respectively in ABAQUS [36].

4.3.3 Element type and mesh sensitivity

The built-up columns, consisting of lipped channel sections as chord members and spacer elements, were modelled using the thin, shear-flexible, isometric quadrilateral shell element S4R available in the ABAQUS library [36]. The channel sections and spacer channels were modelled using the linear 4-node quadrilateral thick shell element S4R, which has six degrees of freedom per node. The upper and lower end plates were modelled using rigid quadrilateral shell elements (R3D4).

An element size of 5 mm by 5 mm was determined to be appropriate for back-to-back channels and spacer channels, based on the results of a convergence study. A typical finite element mesh is shown in Figure 4-5.

Figure 4-5: Typical finite element mesh adopted in the study.

4.3.4 Boundary conditions and load procedure

The ABAQUS library's Rigid Body Tie Constraint option was used to simulate the pin with a warping-restrained boundary condition, as illustrated in Figure 4-6. To ensure concentric axial loading, reference points were established at the cross-sectional centroid of the built-up columns at both ends. The reference point at the non-loading end was used to apply the boundary condition.

The back-to-back gapped built-up CFS columns investigated in this study were pin-ended columns, except for the stub column, which was fixed-fixed. To simulate the upper and lower pin-end supports, displacements and rotations (boundary conditions) were assigned to the upper and lower end plates through reference points. The load was applied through the reference point, as shown in Figure 4-6. The distance between the two reference points is the effective length of each specimen between the two hinged supports, and boundary conditions were assigned to both reference points.

The MPC beam connector element available in the ABAQUS library [36] was used to model the screw connections between the spacer channel and the web of the back-to-back channels.

The load was applied incrementally using the modified RIKS method available in the ABAQUS library [36]. The RIKS method is generally capable of predicting unstable and nonlinear collapse behavior, such as post-buckling behavior.

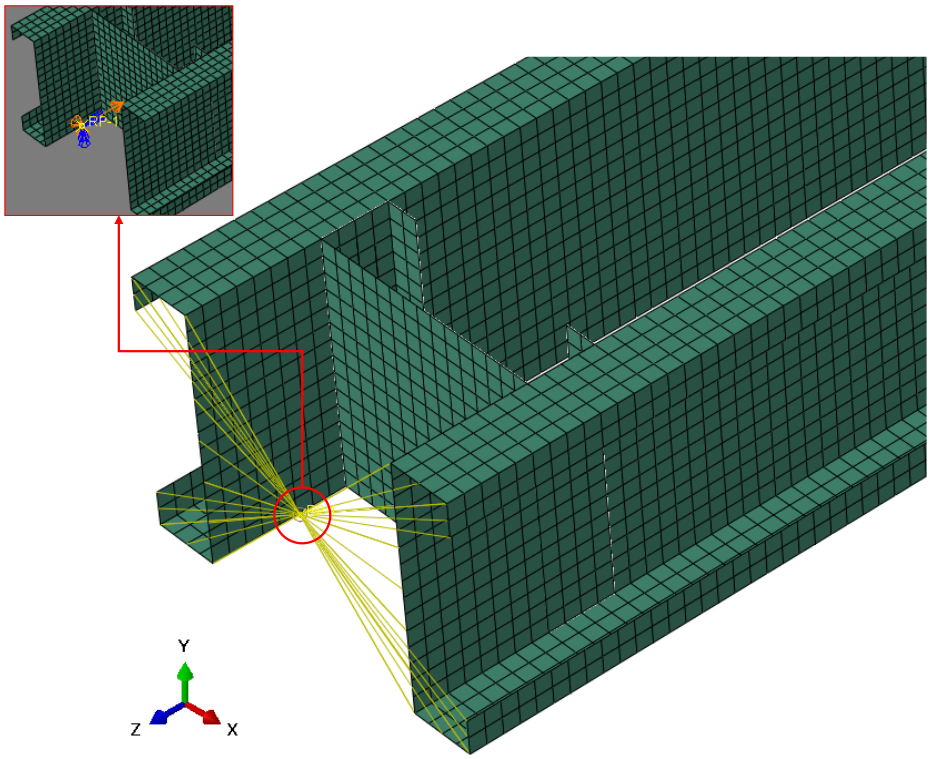

Figure 4-6: Load application through reference point.

4.3.5 Modelling of initial imperfections

The local and flexural buckling behavior of CFS built-up sections depends on several factors, including channel sectional compactness, slenderness around the major/minor axis, and unbraced chord slenderness. Due to the thin-walled nature of CFS sections, the fabrication process induces initial imperfections in CFS built-up members. Therefore, incorporating local and flexural buckling modes is crucial for accurate finite element analysis and was adopted accordingly.

Eigen buckling analyses of the built-up columns were performed to determine the contours for local and flexural buckling imperfections (Figure 4-7). The lowest buckling mode obtained from the linear eigen buckling analysis was used: for short columns, it was the local buckling

mode; for long columns, it was the flexural buckling mode. The lowest mode of each buckling type was adopted for intermediate columns that failed by interactive buckling (local and flexural).

Following the recommendations of Schafer and Pekoz [35], the magnitudes of the local and global imperfections were considered as 0.34 times the thickness (t) and 1/1000 of the full length of the column, respectively. While ABAQUS offers options to incorporate residual stresses, past studies have indicated that including them in numerical analyses significantly affects the failure modes and strength characteristics of CFS built-up members [38-41, 42-44, 45-48, 26]. To avoid complexity in the numerical analysis, residual stresses were not considered.

4.3.6 FE validation

The experimental tests on thin-walled built-up columns conducted by Roy et al. [26] were compared against the test results of back-to-back built-up cold-formed steel (CFS) columns with no gap by Ting et al. [49]. These tests considered CFS double-lipped channels with thicknesses of 1.2 mm, specifically C75 and C90. These channels were placed back-to-back with a gap and connected by respective channels, represented as, for example, GBU75-T1.2-L300-S50. In this notation, GBU75 indicates a double-lipped channel with a width of 75 mm, a flange of 20 mm, and a lip of 10 mm, used to construct a gapped built-up section with a thickness of 1.2 mm (T1.2). The channels have a length of 300 mm (L300) and spacers placed 50 mm apart (S50). Figure 1-2 provides a complete description of all the geometrical dimensions for the specimens.

The specimens, labelled according to the author's system, were compressed between pin-ended supports and had nominal column lengths (L) of 300, 500, 1000, and 2000 mm. The measured yield strength and Young’s modulus of the steel for the 1.2 mm thickness were 565 MPa and 205 GPa, respectively.

The finite element (FE) approach was verified with the built-up column test results reported by Roy et al. [26]. Table 4.1 shows the comparison of experimental values with compressive strengths predicted by the finite element analysis. A close match was obtained between the tests and FE model results in terms of ultimate compression strength and failure modes. The FE results for GBU75 and GBU90 channels, with lengths from 300 to 2000 mm, showed good agreement with the experimental results. Figures 4-7 to 4-9 illustrate the comparison of failure modes obtained from both the experiment and finite element analysis. Figure 4-7 shows the local buckling of the 300 mm GBU75-T1.2-L300-S50 specimen. Figures 4-8 and 4-9 show Modes A and B from the finite element model, which closely match the experimental results. Figure 4-9 also compares the load-displacement curves from the experiment and finite element analysis, indicating good agreement in compression capacity. However, the stiffness of the load-displacement curve from the finite element analysis is higher than that of the experiment, likely due to the assumption of the screws as perfectly rigid elements.

Experimental

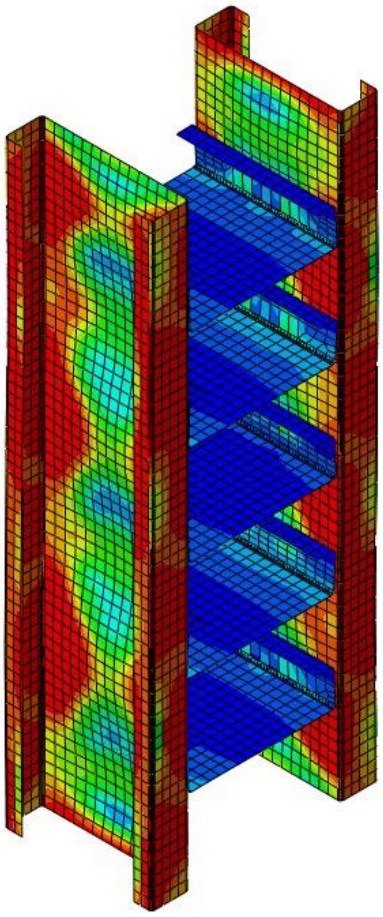

FEA

Figure 4-7: Local Buckling of GBU75-T1.2-L300-S50

Experimental

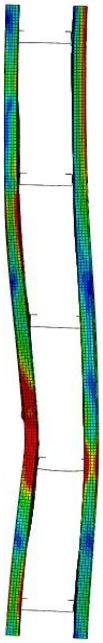

FEA

Figure 4-8: Global Buckling mode of GBU75-T1.2-L1000-S225

Experimental

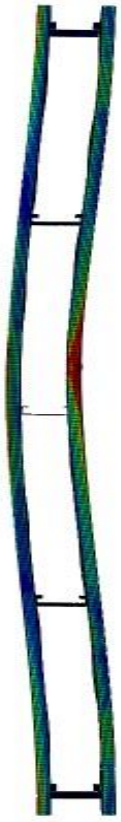

FEA

Figure 4-9: Global Buckling mode of GBU75-T1.2-L2000-S475.

Table 4-1: Comparison of Experimental [1] and Finite Element Analysis for GBU75

Specimen	Web	Flange	Lip	Thickness	Length	Gap between Columns	Spacing	spacers	Experiment Results (P Exp)	FE Results (P FEA)	Ratio (P Exp / P FEA)
	(mm)	(mm)	(mm)	(mm)	(mm)	(mm)	(mm)		(kN)	(kN)	
GBU75-T1.2-L300-S50	75	20	10	1.2	300	75	50	5	122.6	107.04	1.08
GBU75-T1.2-L300-S200	75	20	10	1.2	300	75	200	2	114.3	110.81	1.10
GBU75-T1.2-L500-S100	75	20	10	1.2	500	75	100	5	115.1	103.66	1.00
GBU75-T1.2-L500-S400	75	20	10	1.2	500	75	400	2	101.8	109.35	1.03
GBU75-T1.2-L1000-S225	75	20	10	1.2	1000	75	225	5	77.1	69.97	0.90
GBU75-T1.2-L1000-S900	75	20	10	1.2	1000	75	900	2	65.3	70.38	1.07
GBU75-T1.2-L2000-S475	75	20	10	1.2	2000	75	475	5	25.7	23.06	0.92
GBU75-T1.2-L2000-S1900	75	20	10	1.2	2000	75	1900	2	21.3	26.92	0.95
Mean											1.00
COV											0.072

CHAPTER 5. Parametric Comparison with Design Study and Current Design Rule

The finite element model discussed in the previous section was used to determine the compressive strength for a range of column length (L), section thickness (t), material yield strength, number of spacers, longitudinal spacing of spacers and transverse spacing of columns for back-to-back gapped channel sections of dimensions as shown in Table 2. Further, the compressive strength obtained from the parametric study was used for comparison against the current design rule as per AS/NZS-4600:2018.

Table 2: Parametric Study Values

Parameter	**Values of Parametric study**
Length of the column (mm)(L)	1000, 1500, 2000, 2500, 3000, 3500, 4000
Thickness of section (mm)	0.25, 0.5, 0.75, 1.0, 1.25, 1.5
Material properties (MPa)	565
Number of Spacers	2 to 11 Spacers
Longitudinal spacing of spacers	300, 400, 500, 600, 800, 900, 950
Transverse spacing of columns	0.5G, 0.75G, 1G, 1.5G. (G=Spacer table width/channel width)

5.1 Labelling of specimens

1. For the specimens of **single channel sections**, as plane channels are considered, the nomenclature of specimens are shown as:

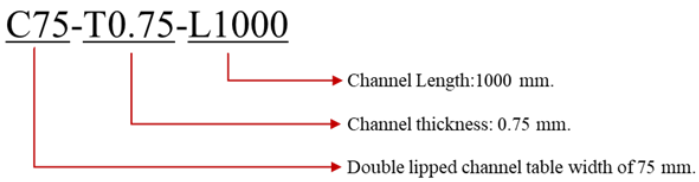

2. For the specimens of built-up sections, as plane channels are considered, the labelling of specimens are shown as:

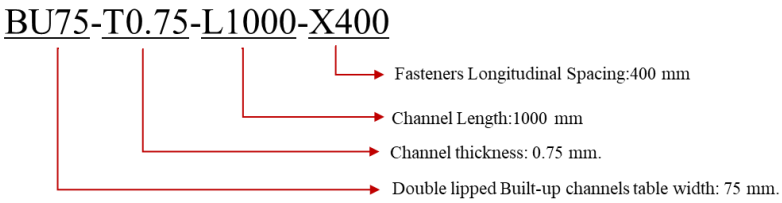

3. For the specimens of **gapped built-up sections**, as plane channels are considered, the labelling of specimens are shown as:

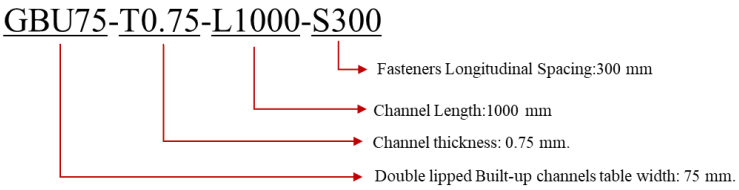

5.2 Results and discussion:

This section presents a detailed discussion of the parametric study carried out on the effect of the number of spacers for different lengths ranging from 1000 to 4000 mm, the effect of transverse spacing of spacers and the comparison of the axial capacity of back-to-back gapped channel sections with single-channel, non-gapped back-to-back, and back-to-back configurations with transverse spacing.

5.2.1 Effect of number of spacers

The number of spacers has been varied from 2 to 11 for a 1000-4000 mm column length to check its effect on the compressive strength of the back-to-back gapped channel. **Error!**

Reference source not found. shows the variation of number of spacers against the compressive strength for GBU75. It has been observed that for 1000 -4000 mm Column lengths of GBU75-T0.75, the Compressive strength is 41.22kN for 1000 mm Length, remained unchanged till 3 spacers and a negligible increase of 42.97kN at 3 pacers and remained constant till 11 spacers. The Column Lengths of 2000, 3000 and 4000mm, compressive strengths at 2 spacers are 14.98, 6.24 and 3.62kN respectively. At 3 spacers, the values are 16.37, 8.11, and 4.40kN respectively and post 3 spacers the variation in compressive strength is insubstantial, which is shown in the figure.

Figure shows the variation of length against the compressive strength of GBU75 column for 3 and 11 spacers. The strength is inversely proportional to length as well as the strength is same for 3 and 11 spacers. It is observed that the average compressive strength variation between 3 and 11 spacers at 1000,1500, 2000, 2500, 3000 mm is 1.03, 1.73, 0.54, 0.49, and 0.41kN respectively and percentage variation decreases from 4.24 to 0 through different specified lengths.

Additionally, it has also been observed that at the odd number of spacers, the strength is more when compared to the even number of spacers. GBU75-L2000 is taken and analysed compression strength for an even number of spacers from 2-20 and an odd number of spacers from 3-19, observed that the compressive strength variation between 2 and 3 is 1.82kN and variation percentage observed to be 12.5%. Compressive strength variation between 4 and 5 is 1.03kN and variation percentage is observed to be 6.7%. The variations exist but are minimal when observed after 5 spacers. variation between 17 and 18 is 0.05kN and variation percentage is observed to be 0.29% and both the variation and percentage variation between 19 and 20 is equal to 0. The compressive strength increases up to 3 spacers and further plateaus. The reason is that the incorporation of the spacers curtailed the local buckling half-wavelength of the slender elements that form the built-up cross-section, resulting in the development of higher

buckling resistance, particularly for columns failing by local buckling. However, beyond the three spacers, this doesn't give any further benefit.

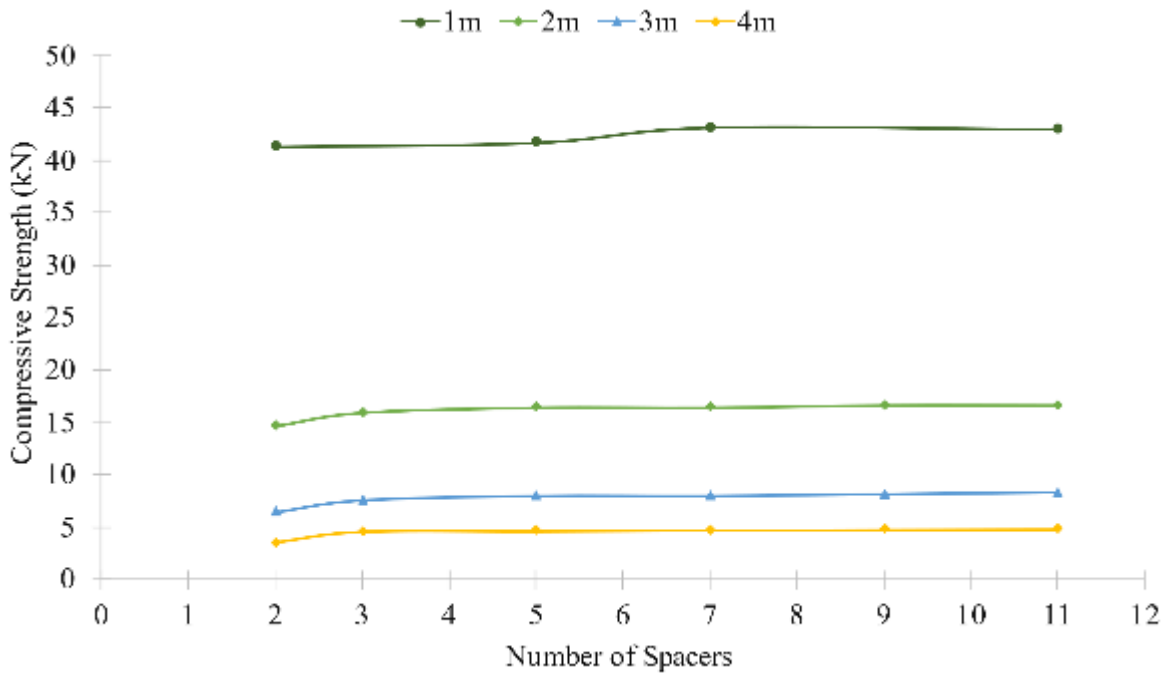

Figure 5-1: Variation of number of spacers against strength for GBU75

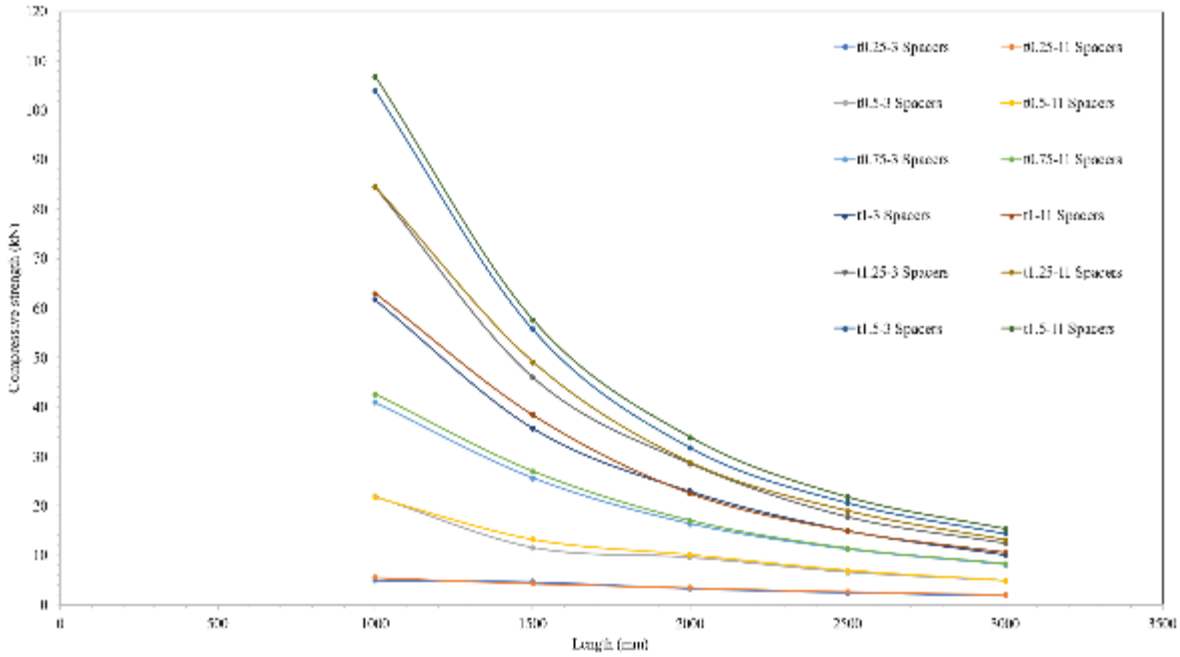

Figure 5-2: Variation of strength against length for GBU 75 column with 3 and 11 spacers.

5.2.2 Effect of Thickness for single, back-to-back and back-to-back gapped channel sections

The section undertakes the comparison of axial compression capacities of various channel thicknesses ranging from 0.25 to 1.5 mm of single, back-to-back and back-to-back gapped channel sections.

The analysis covers the axial compression capacity data ranging from 0.25 to 1.5 mm in channel thickness.

It is observed that the axial capacity of the channel sections demonstrates a progressive inclination with the increase of channel thickness. The percentage increase in axial capacity for single channel C75 thickness ranging from 0.25 to 1.5 mm for channel length of 1000 mm is 0, 68.81, 111.46, 133.29, 149.74and 162.63% respectively, whereas percentage increase of axial capacity for 2000 mm channel length with the same range of thickness is 0, 65.32, 95.82, 117.54, 133.99, 146.90% respectively. The average percentage increase in axial capacity for single channel C75 thickness ranging from 0.25 to 1.5 mm is 0, 63.39, 96.39, 118.06, 134.51, and 147.41% respectively.

The percentage increase in axial capacity for built-up channel BU75 thickness ranging from 0.25 to 1.5 mm for a channel length of 1000 mm is 0, 71.24, 108.99, 136.17, 155.03 and 170.12% respectively, whereas percentage increase of axial capacity for 2000 mm channel length with the same range of thickness is 0, 56.94, 92.03, 115.55, 134.17 and 148.45% respectively. The average percentage increase in axial capacity for single channel BU75 thickness ranging from 0.25 to 1.5 mm is 0, 59.07, 94.47, 119.18, 137.79 and 152.43% respectively.

The percentage increase in axial capacity for built-up channel GBU75 thickness ranging from 0.25 to 1.5 mm for a channel length of 1000 mm is 0, 76.89, 128.19, 154.83, 181.20 and 199.91% respectively, whereas percentage increase of axial capacity for 2000 mm channel length with the same range of thickness is 0, 66.20, 107.27, 135.78, 154.58 and 166.54%

respectively. The average percentage increase in axial capacity for single channel GBU75 thickness ranging from 0.25 to 1.5 mm is 0, 66.58, 104.23, 130.80, 149.16 and 163.11% respectively.

5.2.3 Effect of length for single, back-to-back and back-to-back gapped channel sections

The section undertakes the comparison of axial compression capacities of various channel lengths ranging from 1000 to 3000 mm of single, back-to-back and back-to-back gapped channel sections.

The analysis covers the axial compression capacity data ranging from 1000 to 3000 mm Channel lengths against 0.25 to 1.5 mm in channel thickness.

It is observed that the axial capacity of the channel sections demonstrates a progressive declination with the increase of channel length. The percentage decrease in axial capacity for single channel lengths of C75 ranging from 1000 to 3000 mm for channel thickness of 0.25 to 0.5 mm is 68.81, 67.60, 65.32, 62.29 and 47.92% respectively, whereas the percentage increase of axial capacity for 0.75-1.0 mm channel thickness with the same range of channel length is 133.29, 124.85, 117.54, 114.48 and 100.12% respectively. The average percentage increase in axial capacity for a single channel length of C75 ranging from 1000 to 3000 mm is 125.18, 119.21, 111.92, 108.86 and 94.51% respectively.

The percentage decrease in axial capacity for built-up channel length BU75 ranging from 1000 to 3000 mm for channel thickness of 0.25 to 0.5 mm is 71.24, 60.51, 56.94, 54.02 and 52.67% respectively, whereas percentage increase of axial capacity for 0.75-1.0 mm channel thickness with the same range of channel length is 136.17, 121.49, 115.55, 112.45 and 110.22% respectively. The average percentage increase in axial capacity for a built-up channel length of BU75 ranges from 1000 to 3000 mm 128.31, 114.88, 109.43, 105.98 and 104.34% respectively.

The percentage decrease in axial capacity for built-up channel length GBU75 ranging from 1000 to 3000 mm for channel thickness of 0.25 to 0.5 mm is 76.89, 73.31, 66.20, 65.34 and

60.45% respectively, whereas percentage increase of axial capacity for 0.75-1.0 mm channel thickness with the same range of channel length is 154.83, 139.70, 135.78, 127.00 and 120.72% respectively. The average percentage increase in axial capacity for a built-up channel length of GBU75 ranges from 1000 to 3000 mm 148.20, 131.71, 126.09, 118.61 and 114.69% respectively.

5.2.4 Comparison of FEA of single, back-to-back, and back-to-back gapped channel section with AS/NZS-4600:2018 considering different transverse spacing of back-to-back gapped channel sections

This section undertakes a comparative analysis of the axial compression capacities of back-to-back gapped channel sections (GBU75) equipped with Three equally spaced spacers versus back-to-back channel sections (BU75) with Three uniformly spaced connectors, and a single channel section (C75), across various channel thicknesses: A thickness of 0.25 mm, as illustrated in Figure(a); A thickness of 0.5 mm, as presented in Figure(b); A thickness of 0.75 mm, as presented in Figure(c); A thickness of 1.0 mm, depicted in **Error! Reference source not found.**(d); A thickness of 1.25 mm, shown in **Error! Reference source not found.**(e); A thickness of 1.5 mm, as outlined in **Error! Reference source not found.**(f).

The analysis covers the axial capacity data ranging from 1000 mm to 3000 mm in channel length. It has been empirically observed that the axial capacity of these channels demonstrates a progressive decline with the extension of channel length. The percentage decrease in axial capacities for BU75 are 21.41, 13.01, 11.68, 11.67 and 11.58% respectively for the Channel thickness ranging from 0.25, 0.5, 1, 1.25, and 1.5 mm, whereas for the GBU75 with same channel thickness, the decrease percentage ranging from 35.94, 21, 15.65, 14.12 and 13.37% respectively over the span of channel length ranging from 1000 to 3000mm. Moreover, it is noted that the axial capacity values of the back-to-back gapped channel sections consistently exhibit significantly higher figures in comparison to the back-to-back sections, which maintain

intermediate values. This trend persists across all measured intervals of channel length within the specified range. The percentage variance in axial capacity for 0.25, 0.5, 1, 1.25, 1.5 mm thick GBU75 with BU75 is ranging from 20.55, 50.04, 90.37, 109.78, 119.12% to 102.42, 142.23, 155.09, 153.81, 153.01% throughout channel length ranging from 1000 to 3000mm. **Error! Reference source not found.**5-3 offers a comparative evaluation of the compression capacity values between BU75 channel sections and GBU75 channel sections across varying thicknesses and channel lengths. Observations highlight a marked variance in compression capacity for shorter column lengths, with the disparity diminishing progressively for longer column lengths.

This investigation explores variations in the gap between paired channels and assesses outcomes across different scenarios. The transverse spacing, represented by the parameter 'G', quantifies the ratio of the channel's table width to the spacer's table width. For example, G=0.5 indicates that the spacer's table width (37.5 mm) is half that of the channel's table width (75 mm), while G=2 signifies that the spacer's table width (150 mm) is double that of the channel's table width (75 mm). With a fixed number of three spacers and examination of column lengths ranging from 1000 mm to 3000 mm in 500 mm increments, the graph illustrates compression capacity values corresponding to varied transverse spacing parameters 'G' from 0.5, 1.0 and 1.5.

The analysis also includes a curve representing compression capacity values for single channels across column lengths from 1000 mm to 3000 mm, following AS/NZS 4600:2018 standards. This curve illustrates significant compression capacity enhancements for columns measuring 1000 mm to 1500 mm in length, while columns between 2000 mm and 3000 mm exhibit marginal gains for the specified thicknesses (ranging from 0.25 mm to 1.5 mm). The percentage variance in axial capacity at a 1000 mm channel length for thicknesses of 0.25 mm, 0.5 mm, 0.75 mm, 1 mm, 1.25 mm, and 1.5 mm with G=1 compared to other variants are as follows:

45.82, 57.25, 16.94, 11.03, 43.36, and 6.57% respectively. Similarly, for a 1500 mm channel length, the percentage variance in axial capacities is 26.71, 41.43, 10.87, 7.58, 35.67 and 0.5% respectively. At 2000 mm channel length, the percentage variance in axial capacities is 7.05, 14.54, 12.40, 13.74, 40.08 and 3.99%. These findings demonstrate significant compression capacity improvements from 1000 mm to 1500 mm and gradual diminishments from 2000 mm to 3000 mm.

The analysis indicates that a transverse spacing parameter of G=1 results in substantially higher compression capacities for shorter columns, particularly those at 1000 mm and 1500 mm. However, capacity variations are minimal for longer column lengths, leading to the preliminary conclusion that G=1 offers an optimal solution for back-to-back gapped channel sections. This conclusion is contingent upon further investigations into different material thicknesses ranging from 0.25 mm to 1.5 mm.

In the initial configuration of the back-to-back section, without any gap, the moment of inertia about the X-axis (Ixx) surpasses that about the Y-axis (Iyy), indicating a structural strength biased towards resisting bending in the X-direction. However, with the gradual introduction of a gap, parameterized by 'G' and ranging from 0.5 to 1.5, a significant transformation occurs. As 'G' increases from 0.5 to 1, the moment of inertia about the Y-axis (Iyy) progressively rises, signifying an enhancement in the section's resistance to bending along the Y-direction. At 'G' equals 1, the moment of inertia about the Y-axis (Iyy) equals that about the X-axis (Ixx), achieving equilibrium between the bending resistances in both directions. Further increasing 'G' to 1.5, however, results in a reversal of strength dynamics, making the section weaker against bending in the X-direction compared to the Y-direction. Thus, the strategic introduction of a gap allows for precise control over the section's bending characteristics, optimizing its performance in specific loading scenarios.

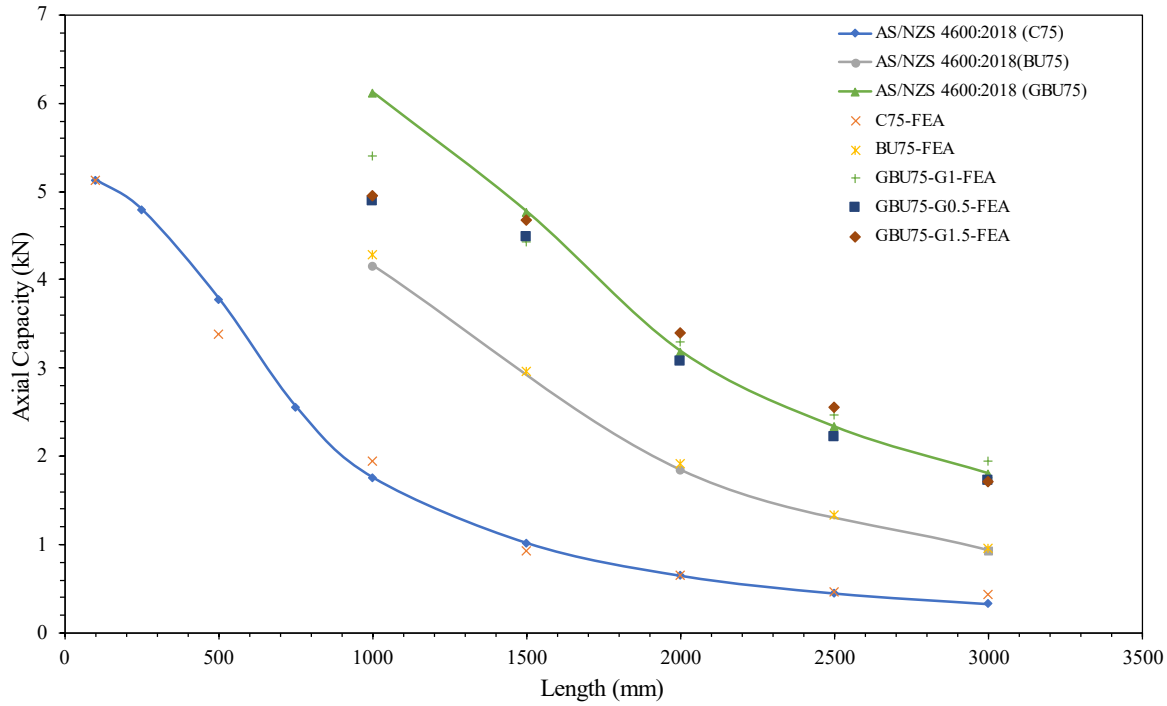
AS/NZS 4600:2018 (C75)
AS/NZS 4600:2018(BU75)
AS/NZS 4600:2018 (GBU75)
C75-FEA
BU75-FEA
GBU75-G1-FEA
GBU75-G0.5-FEA
GBU75-G1.5-FEA
Axial Capacity (kN)
Length (mm)
0
1
2
3
4
5
6
7
0
500
1000
1500
2000
2500
3000
3500

(a)

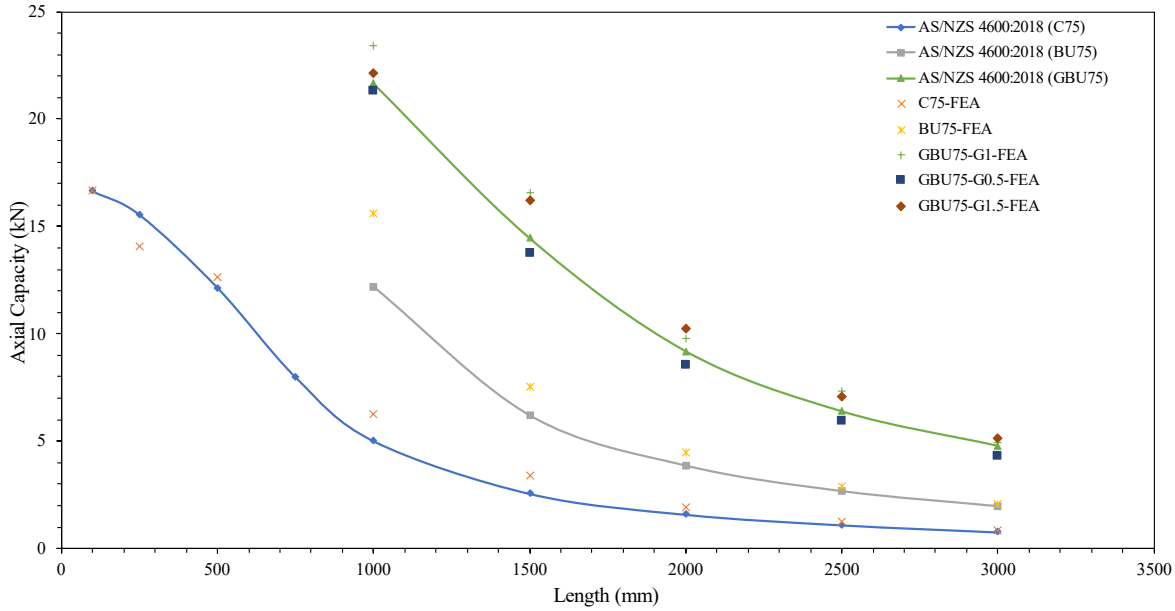
AS/NZS 4600:2018 (C75)
AS/NZS 4600:2018 (BU75)
AS/NZS 4600:2018 (GBU75)
C75-FEA
BU75-FEA
GBU75-G1-FEA
GBU75-G0.5-FEA
GBU75-G1.5-FEA
Axial Capacity (kN)
Length (mm)
0
5
10
15
20
25
0
500
1000
1500
2000
2500
3000
3500

(b)

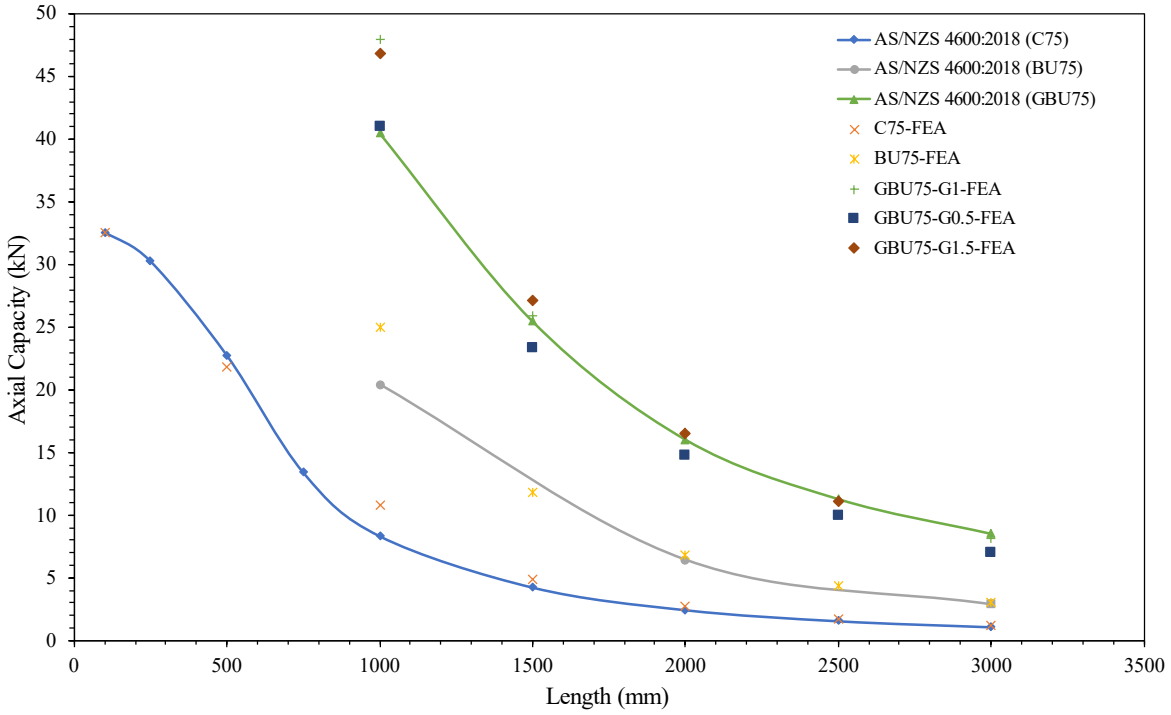
Axial Capacity (kN)
Length (mm)
AS/NZS 4600:2018 (C75)
AS/NZS 4600:2018 (BU75)
AS/NZS 4600:2018 (GBU75)
C75-FEA
BU75-FEA
GBU75-G1-FEA
GBU75-G0.5-FEA
GBU75-G1.5-FEA

(c)

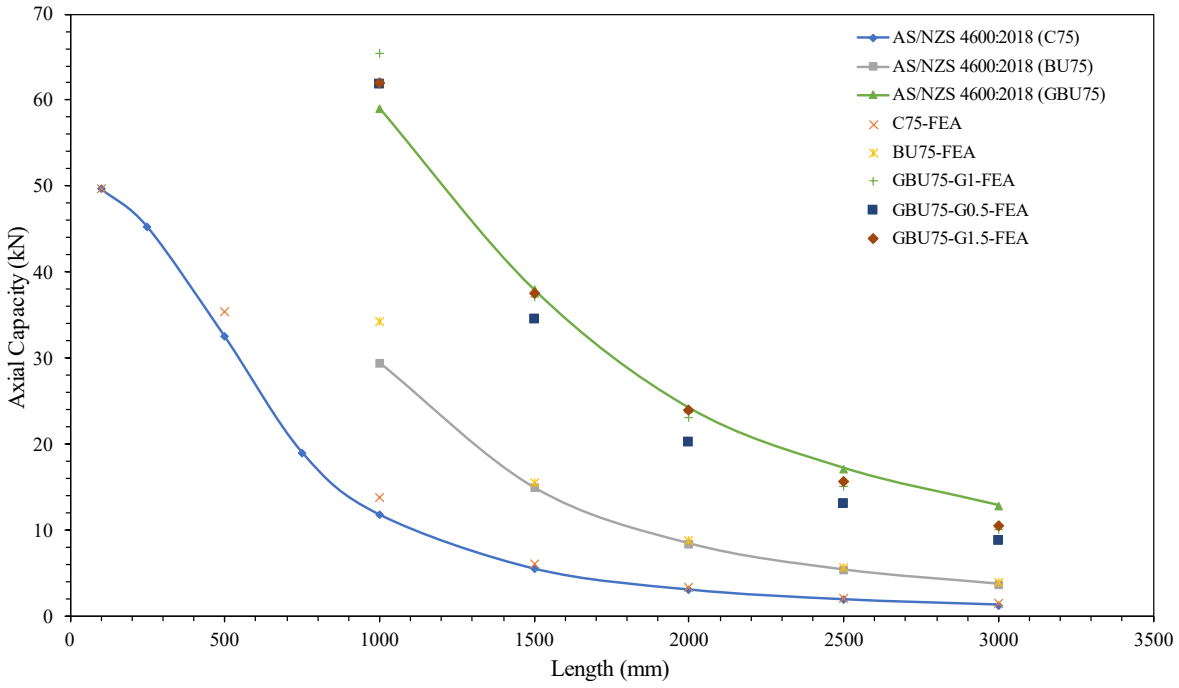
Axial Capacity (kN)
Length (mm)
AS/NZS 4600:2018 (C75)
AS/NZS 4600:2018 (BU75)
AS/NZS 4600:2018 (GBU75)
C75-FEA
BU75-FEA
GBU75-G1-FEA
GBU75-G0.5-FEA
GBU75-G1.5-FEA

(d)

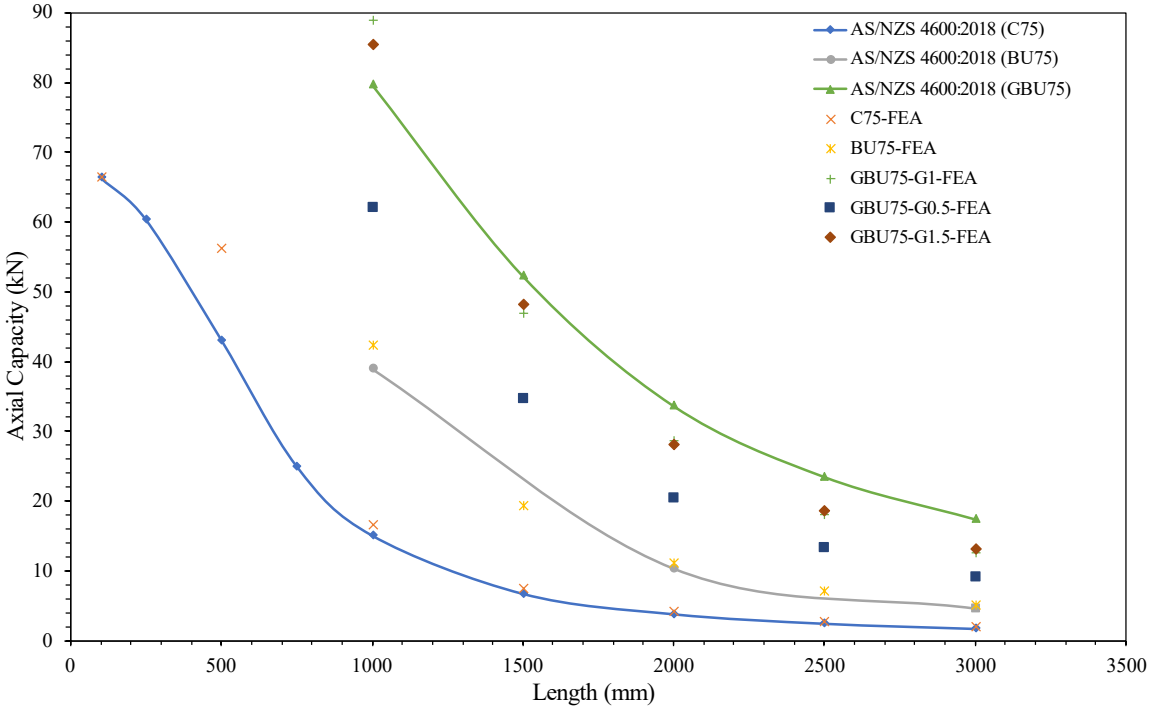

(e)

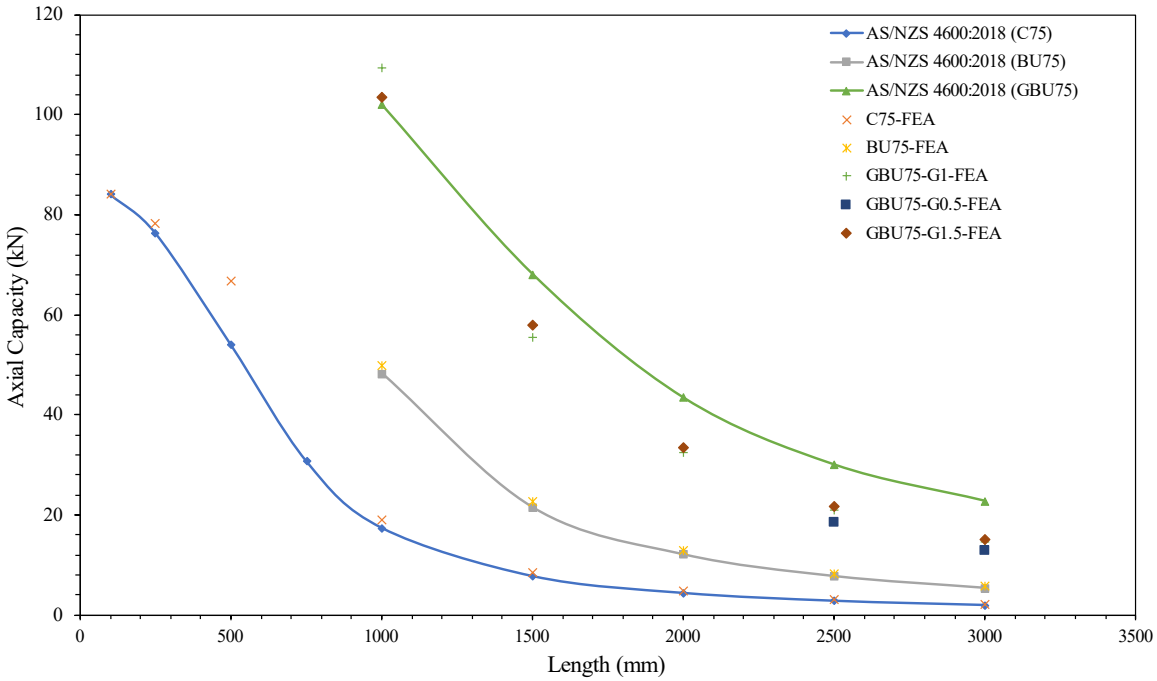

(f)

Figure 5-3: Axial compression capacity of GBU75, BU75 and C75 against AS/NZS 4600:2018 and Cold steel for the thickness of (a) 0.25 mm, (b) 0.50 mm, (c) 0.75 mm, (d) 1.00 mm, (e) 1.25 mm, (f) 1.50 mm.

Similarly, This section undertakes a comparative analysis of the axial compression capacities of back-to-back gapped channel sections (GBU90) equipped with Three equidistant spacers versus back-to-back channel sections (BU90) with Three uniformly spaced connectors, and a single channel section (C90), across various channel thicknesses: A thickness of 0.25 mm, as illustrated in Figure5-4 (a); A thickness of 0.5 mm, as presented in **Error! Reference source not found.**5-4 (b); A thickness of 0.75 mm, depicted in **Error! Reference source not found.**4 (c): A thickness of 1.0 mm, depicted in **Error! Reference source not found.**5-4(d); A thickness of 1.25 mm, shown in **Error! Reference source not found.**5-4 (e); A thickness of 1.5 mm, as outlined in **Error! Reference source not found.**5-4 (f).

The analysis covers the axial capacity data ranging from 1000 mm to 3000 mm in channel length. It has been empirically observed that the axial capacity of these channels demonstrates a progressive decline with the extension of channel length. The percentage decrease in axial capacity for BU90 is 29.44, 60.34, 49.55, 44.51, 36.65, 31.59% respectively for the Channel thickness ranging from 0.25, 0.5, 0.75, 1, 1.25, 1.5 mm, whereas for the GBU90 with same channel thickness, the decrease percentage ranging from 38.91, 61.37, 58.49, 51.25, 50.85, 47.22% respectively for channel length ranging from 1000 to 3000mm. Moreover, it is noted that the axial capacity values of the back-to-back gapped channel sections consistently exhibit significantly higher figures in comparison to the back-to-back sections, which maintain intermediate values. This trend persists across all measured intervals of channel length within the specified range. The percentage variance in axial capacity for 0.25, 0.5, 0.75, 1, 1.25, 1.5 mm thick GBU90 with BU90 is ranging from 43.72, 10.29, 3.58, 12.76, 8.8, 6.77% to 89.93, 12.18, 22.26, 29.84, 50.95, 59.58% for channel length ranging from 1000 to 3000mm. Observations highlight a marked variance in compression capacity for shorter column lengths, with the disparity diminishing progressively for longer column lengths.

Error! Reference source not found. also illustrates the effect of modifying the transverse spacing between channels on the compression capacity of GBU90 transversely spaced channel sections for thickness ranging from 0.25 to 1.5mm. This investigation varies the gap between the paired channels and evaluates the outcomes across different scenarios. The transverse spacing, denoted by the parameter 'G', is defined as the ratio of the channel's table width to the spacer's table width. For instance, a value of G=0.5 indicates that the width of the spacer table (45 mm) is half that of the channel table width (90 mm), while G=2 signifies that the spacer table width (180 mm) is twice the channel table width (90 mm). With a constant number of Three spacers and examining column lengths ranging from 1000 mm to 3000 mm in 500 mm increments, the graph plots compression capacity values corresponding to varying transverse spacing parameter 'G' from 0.5 to 1.5. Additionally, the graphs depict a curve representing the compression capacity values for single channels across column lengths from 100 mm to 3000 mm, as per AS/NZS 4600:2018 standards. This curve shows significant compression capacity improvements for columns measuring 1000 mm to 1500 mm in length, while columns between 2000 mm and 3000 mm exhibit minimal gains for the above-mentioned thickness (from 0.25 to 1.5mm). The percentage variance in axial capacity of 1000 mm channel length for 0.25, 0.5, 0.75, 1, 1.25 and 1.5 mm thick GBU90, G=1 with other variants are 2.85, 39.34, 10.61, 73.17, 0.75 and 3% respectively and the same at 1500mm are 10.48, 48.88, 11.67, 23.73, 19.67 and 0.57% respectively, while at 3000mm the percentage variance in axial capacities are 0.5, 0.55, 4.82, 12.36, 7.73 and 8.82%, which shows a considerable improvement of compression capacities at 1000 to 1500 mm and gradual diminishing from 2000mm to 3000mm. The analysis reveals that a transverse spacing parameter of G=1 yields considerably higher compression capacities for shorter columns, particularly those at 1000 mm and 1500 mm. However, for longer column lengths, the variations in capacity are minimal, leading to the preliminary conclusion that G=1 offers an optimal solution for back-to-back gapped channel

sections. This conclusion is subject to completed investigations into different material thicknesses from 0.25 mm to 1.5 mm.

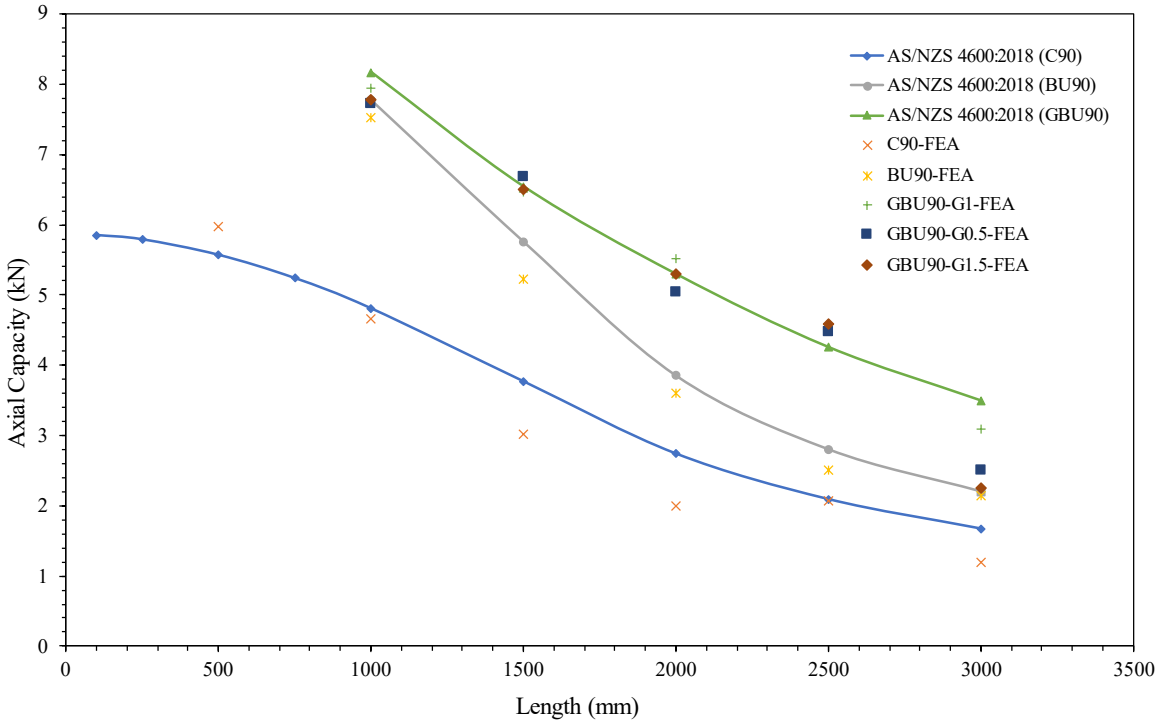
AS/NZS 4600:2018 (C90)
AS/NZS 4600:2018 (BU90)
AS/NZS 4600:2018 (GBU90)
C90-FEA
BU90-FEA
GBU90-G1-FEA
GBU90-G0.5-FEA
GBU90-G1.5-FEA
Axial Capacity (kN)
Length (mm)
0
1
2
3
4
5
6
7
8
9
0
500
1000
1500
2000
2500
3000
3500

(a)

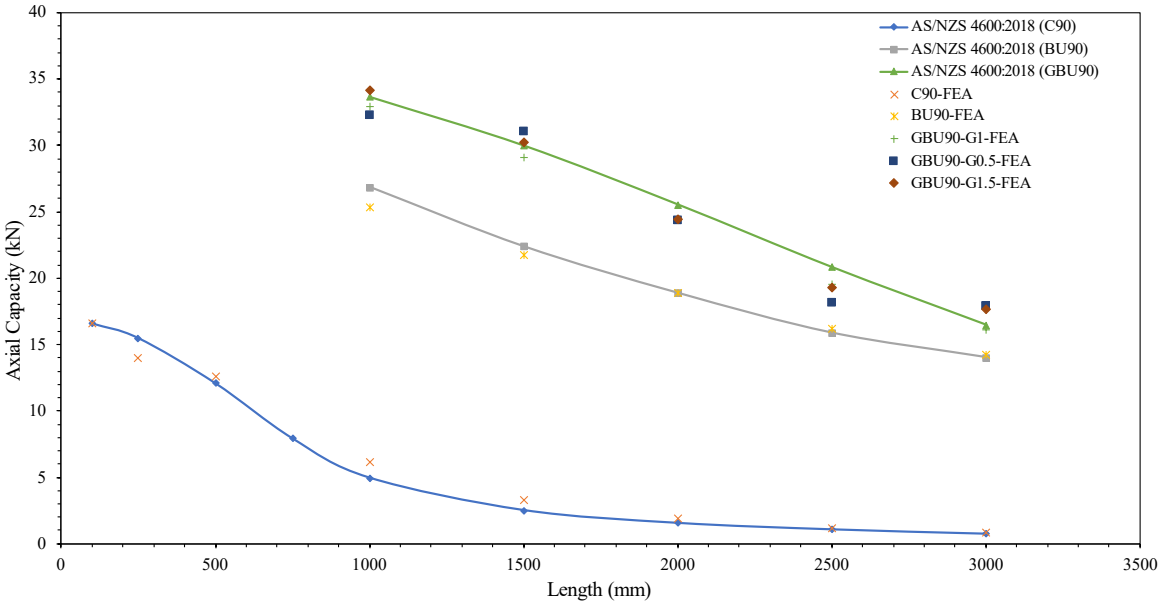
AS/NZS 4600:2018 (C90)
AS/NZS 4600:2018 (BU90)
AS/NZS 4600:2018 (GBU90)
C90-FEA
BU90-FEA
GBU90-G1-FEA
GBU90-G0.5-FEA
GBU90-G1.5-FEA
Axial Capacity (kN)
Length (mm)
0
5
10
15
20
25
30
35
40
0
500
1000
1500
2000
2500
3000
3500

(b)

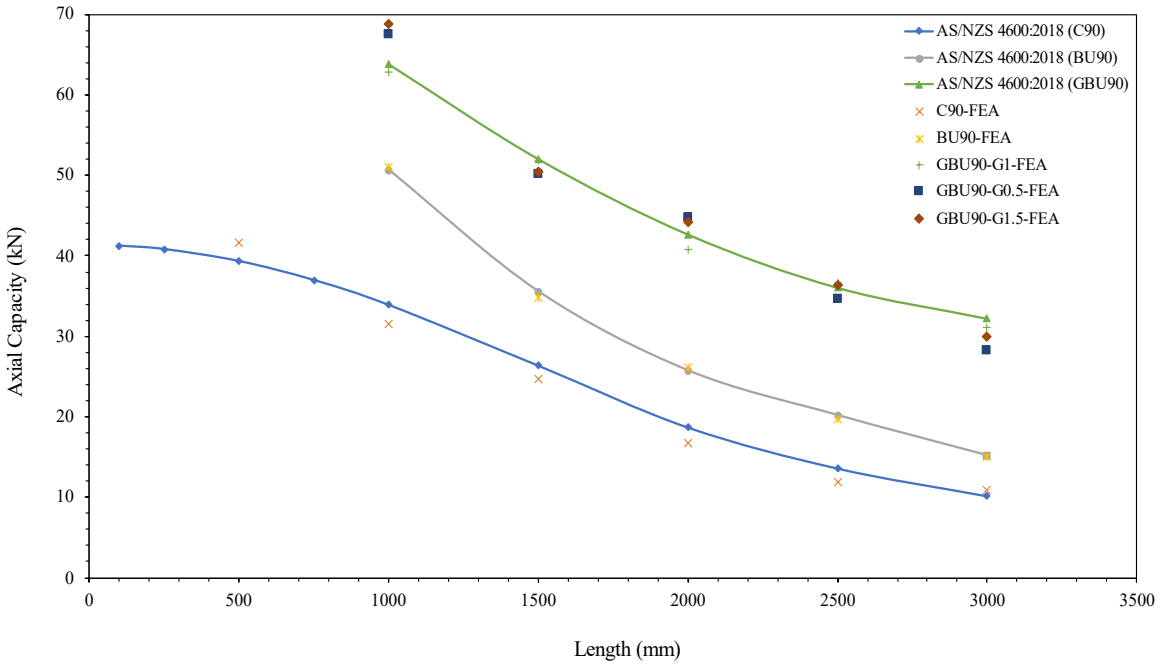
AS/NZS 4600:2018 (C90)
AS/NZS 4600:2018 (BU90)
AS/NZS 4600:2018 (GBU90)
C90-FEA
BU90-FEA
GBU90-G1-FEA
GBU90-G0.5-FEA
GBU90-G1.5-FEA
Axial Capacity (kN)
Length (mm)
0
10
20
30
40
50
60
70
0
500
1000
1500
2000
2500
3000
3500

(c)

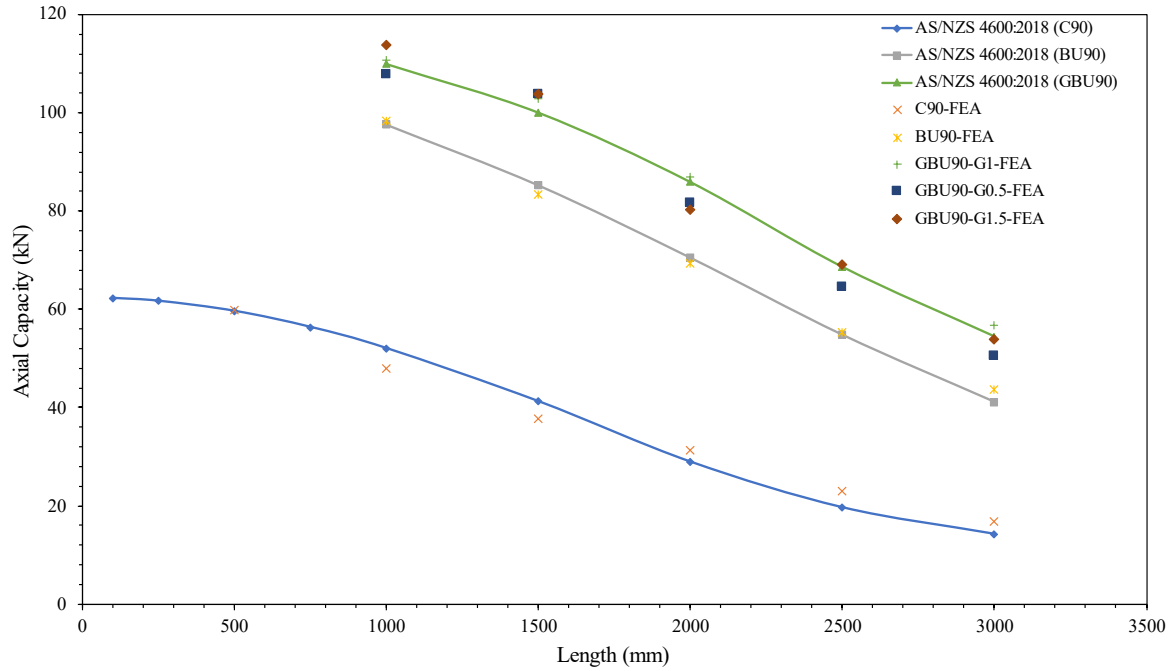
AS/NZS 4600:2018 (C90)
AS/NZS 4600:2018 (BU90)
AS/NZS 4600:2018 (GBU90)
C90-FEA
BU90-FEA
GBU90-G1-FEA
GBU90-G0.5-FEA
GBU90-G1.5-FEA
Axial Capacity (kN)
Length (mm)
0
20
40
60
80
100
120
0
500
1000
1500
2000
2500
3000
3500

(d)

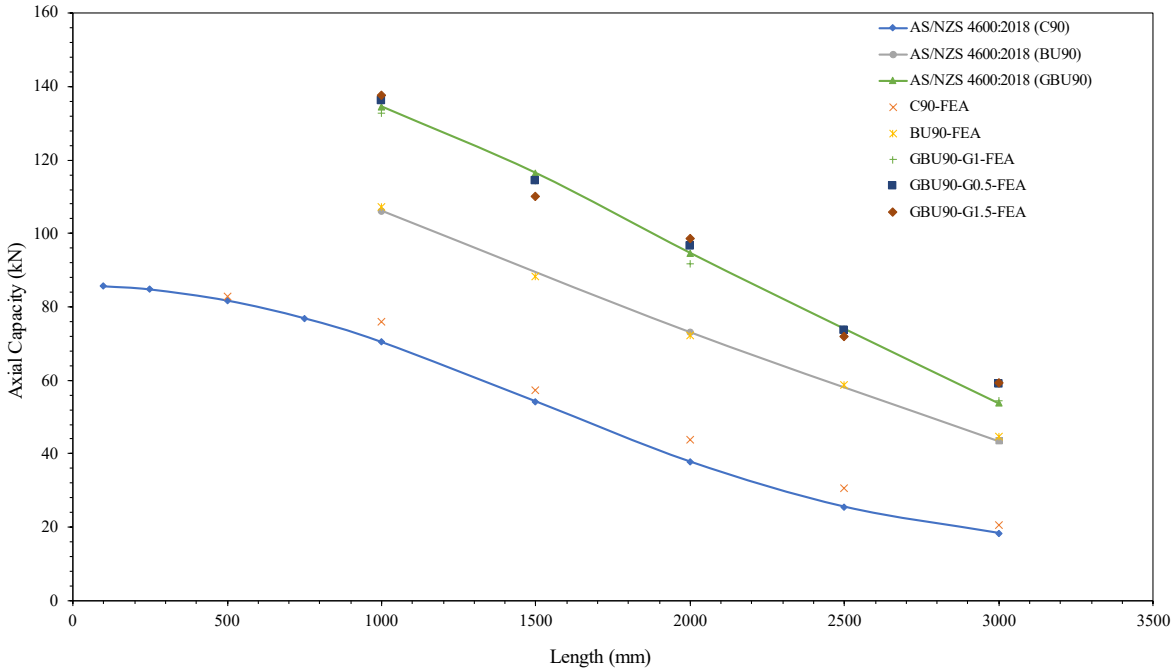

(e)

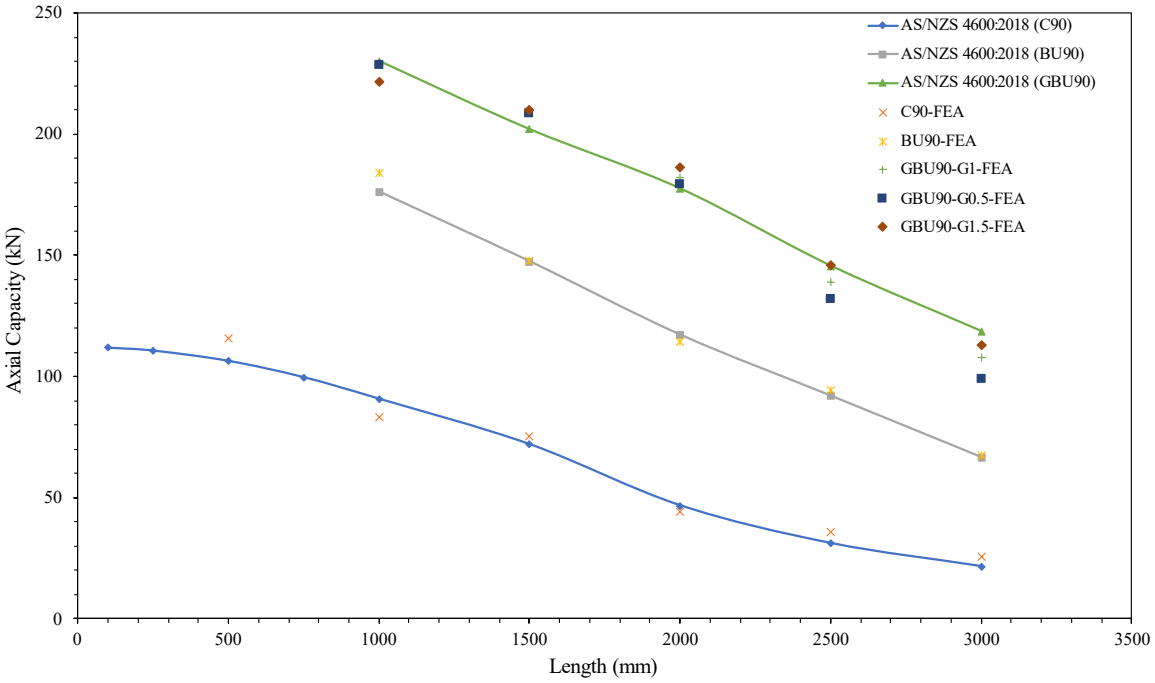

(f)

Figure 5-4: Axial compression capacity of GBU90, BU90 and C90 against AS/NZS 4600:2018 and Cold steel for the thickness of (a) 0.25 mm, (b) 0.50 mm, (c) 0.75 mm, (d) 1.00 mm, (e) 1.25 mm, (f) 1.50 mm.

5.3 Summary of Parametric study:

- A detailed parametric study comprising 1000 validated FE models was conducted to investigate the effects of column length, CFS section thickness, channel materials, spacing between the spacers or number of spacers on the axial capacity of CFS gapped back-to-back channel sections.
- Parameters of channel sections considered as below given table

Length of the column (mm)(L)	1000, 1500, 2000, 2500, 3000, 3500, 4000
Thickness of section (mm)	0.25, 0.5, 0.75, 1.0, 1.25, 1.5
Material properties (MPa)	565
Number of Spacers	2 to 11 Spacers
Longitudinal spacing of spacers	300, 400, 500, 600, 800, 900, 950
Transverse spacing of columns	0.5G, 0.75G, 1G, 1.5G. (G= Spacer table width/channel width)

- Parametric study shows that more than 3 spacers do not affect compressive strength, spacing between channels is sufficient when equal to web depth, and the strength of gapped sections are double that of non-gapped and 4 times for single channel sections.

CHAPTER 6. Conclusions, Limitations and Future Recommendations

6.1 Conclusions

A numerical study was conducted on cold-formed steel (CFS) gapped built-up columns made of lipped channels connected by spacers. A non-linear finite element model was developed and validated against existing test results from the literature. The lipped channel dimensions adhered to the compactness limits specified in Australian/New Zealand Standards (AS/NZ 4600:2018). Various parametric studies were carried out on single-channel CFS columns and built-up columns with different configurations: without gaps, with gaps and three or five spacers, with transverse spacings ranging from 0.5 to 1.5 times the channel web depth, and thicknesses from 0.25 mm to 1.5 mm. FEA results were then compared with the compressive strengths calculated from the current design standards.

Key findings include:

1. For gapped built-up sections in columns up to 4000 mm long, three equally spaced spacers are optimal.

2. The best spacing between channel sections in gapped sections is equal to the channel web depth; increasing this spacing further does not significantly enhance strength.

3. Back-to-back gapped sections show an average 424% increase in compressive strength compared to single-channel configurations, and a 125% improvement over back-to-back non-gapped sections.

4. The FEA results closely match predictions from AS/NZS-4600:2018, with a difference of only 5% in compressive strength.

6.2 Limitations

Channel Sections Considered for FEA:

In this study, only C75 and C90 channel sections were considered. These sections were chosen for their defined geometrical and material properties, including yield strength.

Channel Length Considerations:

Channel lengths ranging from 1000 mm to 3000 mm were considered. These variations help understand how structural performance varies with span length.

Material Specification:

The material used was CFS (Cold-Formed Steel) with a specified yield strength of 565 MPa and Young's Modulus of 205 GPa.

In summary, the instance described involves Finite Element Analysis (FEA) of C75 and C90 channel sections made of CFS with a yield strength and Young's Modulus of 565 MPa., and 205 GPa. respectively. The analysis considers channel lengths ranging from 1000 mm to 3000 mm, with potential extensions to lengths up to 5000 mm, and future possibilities to include CFSS or aluminium channel sections. Each of these factors plays a crucial role in ensuring that the structural design meets performance requirements and optimizes material usage based on specific project needs and constraints.

6.3 Future Recommendations

6.3.1 Study under cyclic loading to understand the connection behaviour between channel and spacer and how that affects the axial capacity:

Studies that analyse the connection behaviour between channels and spacers under cyclic loading and its effect on axial capacity, researchers typically use experimental and analytical methods to investigate the performance of these connections. The connection behaviour is vital because it directly influences the overall stability and load-bearing capacity of the structure. Researchers focus on key points like experimental testing, Analytical Modelling, and Failure Mechanisms, is affect while studying the topic

By studying the connection behaviour between channels and spacers under cyclic loading, researchers aim to improve the understanding of how these elements interact and influence the overall performance of the structure. This knowledge can lead to safer and more efficient designs in various engineering applications. Additionally, although 3 is sufficient in static compression, the effect of the number of spacers should be checked in cyclic loading as well.

6.3.2 Modelling back-to-back gapped sections in trusses to see the overall behaviour of the structure in overall scale Optimization of back-to-back gapped section subjected to static compression:

Studying the modelling of back-to-back gapped sections in trusses to understand the overall behaviour of structures on a macro scale is a common research topic in structural engineering. This analysis is important for assessing the structural integrity, load-carrying capacity, and stability of truss systems under various loading conditions.

By investigating the modelling of back-to-back gapped sections in trusses, researchers aim to enhance the understanding of how these design features impact the overall behaviour and performance of truss structures. This knowledge contributes to the development of more robust and reliable structural designs in civil engineering applications.

6.3.3 Optimization for section size, thickness, and number of spacers of back-to-back gapped section subjected to static compression:

Optimizing back-to-back gapped sections under static compression involves a comprehensive approach focusing on section size, thickness, and spacer configuration. The objective is to enhance load-bearing capacity and structural efficiency while minimizing material usage. This optimization process begins with analytical modelling to define material properties and geometric configurations, followed by applying parametric studies and numerical simulations such as Finite Element Analysis (FEA) to evaluate different design scenarios. Through iterative refinement, optimal dimensions for section size, thickness, and spacer placement are identified to achieve desired strength-to-weight ratios and structural stability.

Experimental validation plays a crucial role in verifying theoretical predictions, where prototypes are tested to measure load-displacement characteristics and validate simulation outcomes. Findings from both theoretical and experimental analyses inform final recommendations for optimal design parameters, documented in detailed technical reports for academic and practical applications. This systematic approach ensures that back-to-back gapped sections are efficiently designed to withstand static compression while meeting performance criteria and maximizing structural integrity.

References

[1] G. Mohaned, Axial load capacity of cold-formed steel built-up stub columns, Int. J. Steel Struct. 17 (4) (2017) 1273–1283.

[2] Son. Tung. Vy, Mahen. Mahendran, T. Sivaprakasam, Built-up back-to-back cold formed steel compression members failing by local and distortional buckling, Thin Walled Struct. 159 (2) (2021) 107224.

[3] Yan Lu, Tianhua Zhou, Wenchao Li, Hanheng Wu, Experimental investigation and a novel direct strength method for cold-formed built-up I section columns, Thin-Walled Struct. 112 (3) (2017) 125–139.

[4] Liu Jui-Ling, D.M. Lue, C.H. Lin, Investigation on slenderness ratios of built-up compression members, J. Construct. Steel Res. 65 (1) (2009) 237–248.

[5] Yaohui Chi, Krishanu Roy, Boshan Chen, et al., Effect of web hole spacing on axial capacity of back-to-back cold-formed steel channels with edge-stiffened holes, Steel Compos. Struct. 40 (7) (2021) 287–305.

[6] Wang Liping, Ben Young, Behavior of cold-formed steel built-up sections with intermediate stiffeners under bending. I: Tests and numerical validation, J. Struct. Eng., ASCE 142 (3) (2016) 1–9.

[7] Qiu-Yun Li, Ben Young, Tests of cold-formed steel built-up open section members under eccentric compressive load, J. Construct. Steel Res. 184 (9) (2021) 106775.

[8] Qiu-Yun Li, Ben Young, Experimental and numerical investigation on cold-formed steel built-up section pin-ended columns, Thin-Walled Struct. 170 (1) (2022) 108444.

[9] Li Q, Young B. Design of cold-formed steel built-up open section members under combined compression and bending[J]. Thin Walled Struct 2022; 172:108890.

[10] Fratamico DC, Turabian S, Zhao X, et al. Experiments on the global buckling and collapse of built-up cold-formed steel columns[J]. J Constr Steel Res 2018;144: 65–80.

[11] Smail Kechidi, David C. Fratamico, Benjamin W. Schafer, et al., Simulation of screw connected built-up cold-formed steel back-to back lipped channels under axial compression, Eng. Struct. 206 (3) (2020) 110109.

[12] Mahar, A. M., Jayachandran, S. A., & Mahendran, M. (2022). Design of locally buckling cold-formed steel built-up columns formed by unlipped channel sections. Thin-Walled Structures, 174, 109132.

[13] Roy, K., Ting, T. C. H., Lau, H. H., & Lim, J. B. (2018, November). Effect of thickness on the behaviour of axially loaded back-to-back cold-formed steel built-up channel sections-Experimental and numerical investigation. In Structures (Vol. 16, pp. 327-346). Elsevier.

[14] Zhou T, Li Y, Wu H, et al. Analysis to determine flexural buckling of cold-formed steel built-up back-to-back section columns[J]. J Constr Steel Res 2020; 166:105898.

[15] Chen B, Roy K, Uzzaman A, et al. Axial strength of back-to-back cold-formed steel channels with edge-stiffened holes, un-stiffened holes, and plain webs[J]. J Constr Steel Res 2020; 174:106313.

[16] Selvaraj S, Madhavan M. Design of cold-formed steel built-up columns subjected to local-global interactive buckling using direct strength method[J]. Thin Walled Struct 2021; 159:107305.

[17] Sang L, Zhou T, Zhang L, et al. Local buckling in cold-formed steel built-up I-section columns: Experiments, numerical validations, and design considerations[J]. Structures 2023; 47:134–52.

[18] Li Q, Young B. Experimental study on cold-formed steel built-up section beam columns experiencing non-uniform bending[J]. Eng Struct 2022; 256:113954.

[19] Qiu-Yun Li, Ben Young, Structural performance of cold-formed steel built-up section beams under non-uniform bending, J. Construct. Steel Res. 189 (1) (2022) 107050.

[20] Li Q, Young B. Numerical investigation, and design of cold-formed steel built-up section beam-column members under moment gradients[J]. Eng Struct 2023;283: 115746.

[21] Zhang J, Young B. Compression tests of cold-formed steel I-shaped open sections with edge and web stiffeners[J]. Thin-Walled Struct 2012; 52:1–11.

[22] Zhang J, Young B. Numerical investigation, and design of cold-formed steel built-up open section columns with longitudinal stiffeners[J]. Thin-Walled Struct 2015; 89:178–91.

[23] He Z, Peng S, Zhou X, et al. Design recommendation of cold-formed steel built-up sections under concentric and eccentric compression[J]. J Constr Steel Res 2024; 212:108255.

[24] Anbarasu M, Venkatesan M. Behavior of cold-formed steel built-up I-section columns composed of four U-profiles. Adv Struct Eng 2019;22(3):613–25.

[25] Ghannam M. Axial Load Capacity of Cold-formed Steel Built-up Stub Columns. Int J Steel Struct 2017;17(3):1–11.

[26] Roy, K., Ting, T. C. H., Lau, H. H., & Lim, J. B. (2018). Nonlinear behaviour of back-to-back gapped built-up cold-formed steel channel sections under compression. Journal of Constructional Steel Research, 147, 257-276.

[27] Anbarasu M, Viyayanand S. Effect of Spacers on Ultimate Strength and Behavior of Cold-Formed Steel Built-up Columns. Proc Eng. 2017; 173:1423–30.

[28] Rondal J, Niazi M. Stability of Built-up Beams and Columns with Thin-Walled Members. J Constr Steel Res. 1990; 16:329–35.

[29] Niazi M. Contribution a L ‘Etude De La Stabilite Des Structures Composees De Profils A Parois Minces Et Section Ouverte De Type C, PhD Thesis-1993, Uni Liege, Belgium (in french).

[30] Rondal J, Niazi M. Stability of Built-up Beams and Columns with Thin-walled members. In: Proc Int Colloquium Stab Steel Struct 1990, Budapest, Hungary.

[31] Crisan A, Ungureanu V, Dubina D. Calibration of Design Formula for Buckling Strength of Built-up back-to-back Cold-formed Steel Members in Compression. In: Proc 7th Int Con Thin-Walled Struct (ICTWS-2014), 2014, Busan, Korea.

[32] Johnston BG. Spaced steel columns. J Struct Div -ASCE 1971;97:1465–79.

[33] Australia/New Zealand Standard (AS/NZS), Cold-Formed Steel Structures, AS/NZS 4600:2018, Standards Australia/Standards New Zealand, 2018.

[34] AISI-S100, North American Specification for the Design of Cold-Formed Steel Structural Members, American Iron and Steel Institute, Washington, D.C, 2016.

[35] M.V.A. Kumar, V. Kalyanaraman, Design strength of locally buckling stub lipped channel columns, J. Struct. Eng. ASCE 138 (2012) 1291–1299.

[36] ABAQUS Analysis User's Manual-Version 6.26, ABAQUS Inc., USA, 2021.

[37] Schafer BW, Pekoz T. Computational modelling of cold-formed steel: characterizing geometric imperfections and residual stresses. J Constr Steel Res 1998;47(3):193–210.

[38] EI Aghoury MA, Salem AH, Hanna MT, Amoush EA. Ultimate capacity of battened columns composed of four equal slender angles. Thin-Walled Struct 2013; 63:175–85.

[39] Dar MA, Sahoo DR, Pulikkal S, Jain AK. Behaviour of laced built-up cold-formed steel columns: experimental investigation and numerical validation. Thin-Walled Struct 2018;132:398–409.

[40] Dar MA, Sahoo DR, Jain AK. Axial compression behavior of laced cold-formed steel built-up columns with unstiffened angle sections. J Constr Steel Res 2019;162. https://doi.org/10.1016/j.jcsr.2019.105727.

[41] Anbarasu M. Behaviour of cold-formed steel built-up battened columns composed of four lipped angles: tests and numerical validation. Adv Struct Eng 2020;23(1):51–64.

[42] Piyawat K, Ramseyer C, Kang TH. Development of an Axial Load Capacity Equation for Doubly Symmetric Built-Up Cold-Formed Sections. J Struct Eng-ASCE 2013;139(12):1–13.

[43] Kesawan S, Mahendran M. Section compression capacity of high strength coldformed hollow flange channels. J Constr Steel Res 2017;133:202–13.

[44] Liu X, Zhou T. Research on axial compression behavior of cold-formed triple-lambs built-up open T-section columns. J Constr Steel Res 2017;134:102–13.

[45] Li Y, Li Y, Wang S, Shen Z. Ultimate load-carrying capacity of cold-formed thin walled columns with built-up box and I section under axial compression. Thin Walled Struct 2014;79:202–17.

[46] Anbarasu M, Kanagarasu K, Sukumar S. Investigation on the behavior and strength of cold-formed steel web stiffened built-up battened columns. Mat Struct 2015;48(12):4029–38.

[47] Dabaon M, Ellobody E, Ramzy K. Nonlinear behavior of built-up cold-formed steel section battened columns. J Constr Steel Res 2015;110:16–28.

[48] Kherbouche S, Megnounif A. Numerical study and design of thin-walled cold formed steel built-up open and closed section columns. Eng Struct. 2019;179(15):670–82.

[49] T.C.H. Ting, K. Roy, H.H. Lau, J.B.P. Lim, Effect of screw spacing on behavior of axially loaded back-to-back cold-formed steel built-up channel sections, Adv. Struct. Eng. 21 (3) (2017) 474–487.

[50] Roy, K., Ting, T. C. H., Lau, H. H., & Lim, J. B. (2018). Cold-Formed Steel Lipped Channel Section Columns Undergoing Local-Overall Buckling Interaction.

[51] DinisP.B. Global–global interaction in cold-formed steel plain and lipped channel columns.

[52] B. Boshra A. El-Taly. Optimization of Cold-Formed Steel Channel Columns.

[53] Anbarasu M., Adil Dar M. Axial capacity of CFS built-up columns comprising of lipped channels with spacers: Nonlinear response and design.

[54] Roy, K., Lim, J. B. Experimental and numerical investigation into the behaviour of face-to-face built-up cold-formed steel channel sections under compression.

[55] Roy, K., Lim, J. B. Effect of screw spacing on behaviour of axially loaded back-to-back cold-formed steel built-up channel sections.

[56] Roy, K., Lim, J. B. Finite Element Modelling of Back-to-Back Built-Up CFS Un-Lipped Channels under Axial Compression.

[57] Zhou T, Li Y. Research on the elastic buckling of composite webs in cold-formed steel back-to-back built-up columns – Part I: Experimental and numerical investigation.

[58] A M Mahar. Global buckling strength of discretely fastened back-to-back built-up cold-formed steel columns.

[59] Dar, A.R., Anbarasu, M., Venkatesan, M. et al. Wide-flanged CFS built-up columns: comparison of test strengths, numerical strengths and design strengths.

Appendix-A

Table A.2: Axial capacity obtained from the parametric study results for CFS channel sections C75-T0.25

Specimen	Web (mm)	Flange (mm)	Lip (mm)	Thickness (mm)	Length (mm)	Fillet radius (mm)	Yield Strength (MPa)	Youngs Modulus (MPa)	AS/NZS-4600:2018 (P) (kN)	FE Results (P FEA) (kN)
C75-T0.25-L100	75	20	10	0.25	100	1.5	565	205000	5.13	5.13
C75-T0.25-L250	75	20	10	0.25	250	1.5	565	205000	4.79	4.45
C75-T0.25-L500	75	20	10	0.25	500	1.5	565	205000	3.78	3.38
C75-T0.25-L750	75	20	10	0.25	750	1.5	565	205000	2.56	2.48
C75-T0.25-L1000	75	20	10	0.25	1000	1.5	565	205000	1.76	1.94
C75-T0.25-L1500	75	20	10	0.25	1500	1.5	565	205000	1.02	0.92
C75-T0.25-L2000	75	20	10	0.25	2000	1.5	565	205000	0.65	0.66
C75-T0.25-L2500	75	20	10	0.25	2500	1.5	565	205000	0.45	0.46
C75-T0.25-L3000	75	20	10	0.25	3000	1.5	565	205000	0.33	0.44
C75-T0.25-L3500	75	20	10	0.25	3500	1.5	565	205000	0.26	0.25
C75-T0.25-L4000	75	20	10	0.25	4000	1.5	565	205000	0.20	0.19
C75-T0.25-L4500	75	20	10	0.25	4500	1.5	565	205000	0.17	0.16
C75-T0.25-L5000	75	20	10	0.25	5000	1.5	565	205000	0.14	5.13

Table A.3: Axial capacity obtained from the parametric study results for CFS channel sections C75-T0.5

Specimen	Web (mm)	Flange (mm)	Lip (mm)	Thickness (mm)	Length (mm)	Fillet radius (mm)	Yield Strength (MPa)	Youngs Modulus (MPa)	AS/NZS-4600:2018 (P) (kN)	FE Results (P FEA) (kN)
C75-T0.5-L100	75	20	10	0.5	100	1.5	565	205000	16.63	16.63
C75-T0.5-L250	75	20	10	0.5	250	1.5	565	205000	15.53	14.03
C75-T0.5-L500	75	20	10	0.5	500	1.5	565	205000	12.13	14.65
C75-T0.5-L750	75	20	10	0.5	750	1.5	565	205000	7.97	8.82
C75-T0.5-L1000	75	20	10	0.5	1000	1.5	565	205000	5.00	6.22
C75-T0.5-L1500	75	20	10	0.5	1500	1.5	565	205000	2.55	3.37
C75-T0.5-L2000	75	20	10	0.5	2000	1.5	565	205000	1.58	1.90
C75-T0.5-L2500	75	20	10	0.5	2500	1.5	565	205000	1.09	1.22
C75-T0.5-L3000	75	20	10	0.5	3000	1.5	565	205000	0.76	0.85
C75-T0.5-L3500	75	20	10	0.5	3500	1.5	565	205000	0.55	0.63
C75-T0.5-L4000	75	20	10	0.5	4000	1.5	565	205000	0.42	0.48

C75-T0.5-L4500	75	20	10	0.5	4500	1.5	565	205000	0.34	0.35
C75-T0.5-L5000	75	20	10	0.5	5000	1.5	565	205000	0.27	0.28

Table A.4: Axial capacity obtained from the parametric study results for CFS channel sections C75-T0.75

Specimen	**Web** (mm)	**Flange** (mm)	**Lip** (mm)	**Thickness** (mm)	**Length** (mm)	**Fillet radius** (mm)	**Yield Strength** (MPa)	**Youngs Modulus** (MPa)	**AS/NZS-4600:2018 (P)** (kN)	**FE Results (P FEA)** (kN)
C75-T0.75-L100	75	20	10	0.75	100	1.5	565	205000	32.59	32.59
C75-T0.75-L250	75	20	10	0.75	250	1.5	565	205000	30.26	27.43
C75-T0.75-L500	75	20	10	0.75	500	1.5	565	205000	22.75	21.82
C75-T0.75-L750	75	20	10	0.75	750	1.5	565	205000	13.41	12.65
C75-T0.75-L1000	75	20	10	0.75	1000	1.5	565	205000	8.34	10.84
C75-T0.75-L1500	75	20	10	0.75	1500	1.5	565	205000	4.25	4.84
C75-T0.75-L2000	75	20	10	0.75	2000	1.5	565	205000	2.45	2.73
C75-T0.75-L2500	75	20	10	0.75	2500	1.5	565	205000	1.57	1.75
C75-T0.75-L3000	75	20	10	0.75	3000	1.5	565	205000	1.09	1.22
C75-T0.75-L3500	75	20	10	0.75	3500	1.5	565	205000	0.80	0.78
C75-T0.75-L4000	75	20	10	0.75	4000	1.5	565	205000	0.61	0.60
C75-T0.75-L4500	75	20	10	0.75	4500	1.5	565	205000	0.48	0.47
C75-T0.75-L5000	75	20	10	0.75	5000	1.5	565	205000	0.39	0.38

Table A.5: Axial capacity obtained from the parametric study results for CFS channel sections C75-T1.00

Specimen	**Web** (mm)	**Flange** (mm)	**Lip** (mm)	**Thickness** (mm)	**Length** (mm)	**Fillet radius** (mm)	**Yield Strength** (MPa)	**Youngs Modulus** (MPa)	**AS/NZS-4600:2018 (P)** (kN)	**FE Results (P FEA)** (kN)
C75-T1.0-L100	75	20	10	0.75	100	1.5	565	205000	49.77	49.77
C75-T1.0-L250	75	20	10	0.75	250	1.5	565	205000	45.34	45.33
C75-T1.0-L500	75	20	10	0.75	500	1.5	565	205000	32.60	35.55
C75-T1.0-L750	75	20	10	0.75	750	1.5	565	205000	19.12	20.23
C75-T1.0-L1000	75	20	10	0.75	1000	1.5	565	205000	11.87	13.87
C75-T1.0-L1500	75	20	10	0.75	1500	1.5	565	205000	5.58	6.19
C75-T1.0-L2000	75	20	10	0.75	2000	1.5	565	205000	3.14	3.49
C75-T1.0-L2500	75	20	10	0.75	2500	1.5	565	205000	2.01	2.24
C75-T1.0-L3000	75	20	10	0.75	3000	1.5	565	205000	1.39	1.55
C75-T1.0-L3500	75	20	10	0.75	3500	1.5	565	205000	1.02	1.12
C75-T1.0-L4000	75	20	10	0.75	4000	1.5	565	205000	0.78	0.82
C75-T1.0-L4500	75	20	10	0.75	4500	1.5	565	205000	0.62	0.63

C75-T1.0-L5000	75	20	10	0.75	5000	1.5	565	205000	0.50	0.48

Table A.6: Axial capacity obtained from the parametric study results for CFS channel sections C75-T1.25

Specimen	**Web** (mm)	**Flange** (mm)	**Lip** (mm)	**Thickness** (mm)	**Length** (mm)	**Fillet radius** (mm)	**Yield Strength** (MPa)	**Youngs Modulus** (MPa)	**AS/NZS-4600:2018 (P)** (kN)	**FE Results (P FEA)** (kN)
C75-T1.25-L100	75	20	10	1.25	100	1.5	565	205000	66.33	66.33
C75-T1.25-L250	75	20	10	1.25	250	1.5	565	205000	60.34	62.43
C75-T1.25-L500	75	20	10	1.25	500	1.5	565	205000	43.10	56.09
C75-T1.25-L750	75	20	10	1.25	750	1.5	565	205000	24.98	25.32
C75-T1.25-L1000	75	20	10	1.25	1000	1.5	565	205000	15.06	16.60
C75-T1.25-L1500	75	20	10	1.25	1500	1.5	565	205000	6.70	7.41
C75-T1.25-L2000	75	20	10	1.25	2000	1.5	565	205000	3.77	4.18
C75-T1.25-L2500	75	20	10	1.25	2500	1.5	565	205000	2.41	2.68
C75-T1.25-L3000	75	20	10	1.25	3000	1.5	565	205000	1.67	1.86
C75-T1.25-L3500	75	20	10	1.25	3500	1.5	565	205000	1.23	1.25
C75-T1.25-L4000	75	20	10	1.25	4000	1.5	565	205000	0.94	1.12
C75-T1.25-L4500	75	20	10	1.25	4500	1.5	565	205000	0.74	0.76
C75-T1.25-L5000	75	20	10	1.25	5000	1.5	565	205000	0.60	0.62

Table A.7: Axial capacity obtained from the parametric study results for CFS channel sections C75-T1.5

Specimen	**Web** (mm)	**Flange** (mm)	**Lip** (mm)	**Thickness** (mm)	**Length** (mm)	**Fillet radius** (mm)	**Yield Strength** (MPa)	**Youngs Modulus** (MPa)	**AS/NZS-4600:2018 (P)** (kN)	**FE Results (P FEA)** (kN)
C75-T1.5-L100	75	20	10	1.5	100	1.5	565	205000	84.07	84.07
C75-T1.5-L250	75	20	10	1.5	250	1.5	565	205000	76.30	78.35
C75-T1.5-L500	75	20	10	1.5	500	1.5	565	205000	53.96	66.63
C75-T1.5-L750	75	20	10	1.5	750	1.5	565	205000	30.69	32.56
C75-T1.5-L1000	75	20	10	1.5	1000	1.5	565	205000	17.35	19.05
C75-T1.5-L1500	75	20	10	1.5	1500	1.5	565	205000	7.71	8.51
C75-T1.5-L2000	75	20	10	1.5	2000	1.5	565	205000	4.34	4.80
C75-T1.5-L2500	75	20	10	1.5	2500	1.5	565	205000	2.78	3.07
C75-T1.5-L3000	75	20	10	1.5	3000	1.5	565	205000	1.93	2.14
C75-T1.5-L3500	75	20	10	1.5	3500	1.5	565	205000	1.42	1.68

C75-T1.5-L4000	75	20	10	1.5	4000	1.5	565	205000	1.08	1.1
C75-T1.5-L4500	75	20	10	1.5	4500	1.5	565	205000	0.86	0.92
C75-T1.5-L5000	75	20	10	1.5	5000	1.5	565	205000	0.69	0.71

Table A.8: Axial capacity obtained from the parametric study results for CFS channel sections BU75-T0.25 to T1.5

Specimen	**Web** (mm)	**Flange** (mm)	**Lip** (mm)	**Thickness** (mm)	**Length** (mm)	**Fillet radius** (mm)	**Spacing** (mm)	**Number of connectors**	**Yield Strength** (MPa)	**Youngs Modulus** (MPa)	**AS/NZS-4600:2018 (P)** (kN)	**FE Results (P FEA)** (kN)
BU75-T0.25-L1000-X450	75	20	10	0.25	1000	1.5	450	3	565	205000	10.99	4.48
BU75-T0.25-L1500-X700	75	20	10	0.25	1500	1.5	700	3	565	205000	2.99	2.97
BU75-T0.25-L2000-X950	75	20	10	0.25	2000	1.5	950	3	565	205000	1.91	1.91
BU75-T0.25-L2500-X1200	75	20	10	0.25	2500	1.5	1200	3	565	205000	1.35	1.33
BU75-T0.25-L3000-X1450	75	20	10	0.25	3000	1.5	1450	3	565	205000	0.97	0.96
BU75-T0.5-L1000-X450	75	20	10	0.5	1000	1.5	450	3	565	205000	21.92	15.58
BU75-T0.5-L1500-X700	75	20	10	0.5	1500	1.5	700	3	565	205000	9.76	7.51
BU75-T0.5-L2000-X950	75	20	10	0.5	2000	1.5	950	3	565	205000	5.49	4.43
BU75-T0.5-L2500-X1200	75	20	10	0.5	2500	1.5	1200	3	565	205000	3.51	2.89
BU75-T0.5-L3000-X1450	75	20	10	0.5	3000	1.5	1450	3	565	205000	2.45	2.03
BU75-T0.75-L1000-X450	75	20	10	0.75	1000	1.5	450	3	565	205000	31.47	25.03
BU75-T0.75-L1500-X700	75	20	10	0.75	1500	1.5	700	3	565	205000	14.05	11.81
BU75-T0.75-L2000-X950	75	20	10	0.75	2000	1.5	950	3	565	205000	7.86	6.83
BU75-T0.75-L2500-X1200	75	20	10	0.75	2500	1.5	1200	3	565	205000	5.06	4.38
BU75-T0.75-L3000-X1450	75	20	10	0.75	3000	1.5	1450	3	565	205000	3.50	3.06
BU75-T1.0-L1000-X450	75	20	10	1.0	1000	1.5	450	3	565	205000	10.99	4.48
BU75-T1.0-L1500-X700	75	20	10	1.0	1500	1.5	700	3	565	205000	2.99	2.97
BU75-T1.0-L2000-X950	75	20	10	1.0	2000	1.5	950	3	565	205000	1.91	1.91
BU75-T1.0-L2500-X1200	75	20	10	1.0	2500	1.5	1200	3	565	205000	1.35	1.33
BU75-T1.0-L3000-X1450	75	20	10	1.0	3000	1.5	1450	3	565	205000	0.97	0.96
BU75-T1.25-L1000-X450	75	20	10	1.25	1000	1.5	450	3	565	205000	21.92	15.58
BU75-T1.25-L1500-X700	75	20	10	1.25	1500	1.5	700	3	565	205000	9.76	7.51
BU75-T1.25-L2000-X950	75	20	10	1.25	2000	1.5	950	3	565	205000	5.49	4.43

BU75-T1.25-L2500-X1200	75	20	10	1.25	2500	1.5	1200	3	565	205000	3.51	2.89
BU75-T1.25-L3000-X1450	75	20	10	1.25	3000	1.5	1450	3	565	205000	2.45	2.03
BU75-T1.5-L1000-X450	75	20	10	1.5	1000	1.5	450	3	565	205000	31.47	25.03
BU75-T1.5-L1500-X700	75	20	10	1.5	1500	1.5	700	3	565	205000	14.05	11.81
BU75-T1.5-L2000-X950	75	20	10	1.5	2000	1.5	950	3	565	205000	7.86	6.83
BU75-T1.5-L2500-X1200	75	20	10	1.5	2500	1.5	1200	3	565	205000	5.06	4.38
BU75-T1.5-L3000-X1450	75	20	10	1.5	3000	1.5	1450	3	565	205000	3.50	3.06

Table A.9: Axial capacity obtained from the parametric study results for CFS channel sections GBU75-T0.25 to T1.5

Specimen	**Web** (mm)	**Flange** (mm)	**Lip** (mm)	**Thickness** (mm)	**Length** (mm)	**Fillet radius** (mm)	**Spacing** (mm)	**Number of connectors**	**Yield Strength** (MPa)	**Youngs Modulus** (MPa)	**AS/NZS-4600:2018 (P)** (kN)	**FE Results (P FEA)** (kN)
GBU75-T0.25-L1000-S450	75	20	10	0.25	1000	1.5	450	3	565	205000	5.47	5.40
GBU75-T0.25-L1500-S700	75	20	10	0.25	1500	1.5	700	3	565	205000	4.44	4.42
GBU75-T0.25-L2000-S950	75	20	10	0.25	2000	1.5	950	3	565	205000	3.37	3.30
GBU75-T0.25-L2500-S1200	75	20	10	0.25	2500	1.5	1200	3	565	205000	2.46	2.47
GBU75-T0.25-L3000-S1450	75	20	10	0.25	3000	1.5	1450	3	565	205000	1.95	1.94
GBU75-T0.5-L1000-S450	75	20	10	0.5	1000	1.5	450	3	565	205000	23.36	23.38
GBU75-T0.5-L1500-S700	75	20	10	0.5	1500	1.5	700	3	565	205000	16.57	16.57
GBU75-T0.5-L2000-S950	75	20	10	0.5	2000	1.5	950	3	565	205000	9.78	9.75
GBU75-T0.5-L2500-S1200	75	20	10	0.5	2500	1.5	1200	3	565	205000	7.34	7.33
GBU75-T0.5-L3000-S1450	75	20	10	0.5	3000	1.5	1450	3	565	205000	4.93	4.91
GBU75-T0.75-L1000-S450	75	20	10	0.75	1000	1.5	450	3	565	205000	48.05	48.01
GBU75-T0.75-L1500-S700	75	20	10	0.75	1500	1.5	700	3	565	205000	25.97	25.88
GBU75-T0.75-L2000-S950	75	20	10	0.75	2000	1.5	950	3	565	205000	16.59	16.58
GBU75-T0.75-L2500-S1200	75	20	10	0.75	2500	1.5	1200	3	565	205000	11.15	11.11
GBU75-T0.75-L3000-S1450	75	20	10	0.75	3000	1.5	1450	3	565	205000	8.18	8.11
GBU75-T1.0-L1000-S450	75	20	10	1.0	1000	1.5	450	3	565	205000	65.71	65.45
GBU75-T1.0-L1500-S700	75	20	10	1.0	1500	1.5	700	3	565	205000	37.34	37.19
GBU75-T1.0-L2000-S950	75	20	10	1.0	2000	1.5	950	3	565	205000	23.29	23.16
GBU75-T1.0-L2500-S1200	75	20	10	1.0	2500	1.5	1200	3	565	205000	15.14	15.14

GBU75-T1.0-L3000-S1450	75	20	10	1.0	3000	1.5	1450	3	565	205000	10.26	10.24
GBU75-T1.25-L1000-S450	75	20	10	1.25	1000	1.5	450	3	565	205000	88.94	88.88
GBU75-T1.25-L1500-S700	75	20	10	1.25	1500	1.5	700	3	565	205000	46.74	46.90
GBU75-T1.25-L2000-S950	75	20	10	1.25	2000	1.5	950	3	565	205000	28.59	28.52
GBU75-T1.25-L2500-S1200	75	20	10	1.25	2500	1.5	1200	3	565	205000	17.99	17.93
GBU75-T1.25-L3000-S1450	75	20	10	1.25	3000	1.5	1450	3	565	205000	12.56	12.55
GBU75-T1.5-L1000-S450	75	20	10	1.5	1000	1.5	450	3	565	205000	109.37	109.34
GBU75-T1.5-L1500-S700	75	20	10	1.5	1500	1.5	700	3	565	205000	55.49	55.46
GBU75-T1.5-L2000-S950	75	20	10	1.5	2000	1.5	950	3	565	205000	33.48	32.40
GBU75-T1.5-L2500-S1200	75	20	10	1.5	2500	1.5	1200	3	565	205000	20.95	20.91
GBU75-T1.5-L3000-S1450	75	20	10	1.5	3000	1.5	1450	3	565	205000	14.68	14.62

Table A.10: Axial capacity obtained from the parametric study results for GBU75-T0.25 to T1.5 with transverse gap (G)=0.5 and 1.5

Specimen	**Web**	**Flange**	**Lip**	**Thickness**	**Length**	**Fillet radius**	**Spacing**	**Number of spacers**	**Yield Strength**	**Youngs Modulus**	**AS/NZS-4600:2018 (P)**	**FE Results (P FEA)**
	(mm)	(mm)	(mm)	(mm)	(mm)	(mm)	(mm)		(MPa)	(MPa)	(kN)	(kN)
GBU75-T0.25-L1000-S450-G0.5	75	20	10	0.25	1000	1.5	450	3	565	205000	5.47	4.89
GBU75-T0.25-L1500-S700-G0.5	75	20	10	0.25	1500	1.5	700	3	565	205000	4.44	4.49
GBU75-T0.25-L2000-S950-G0.5	75	20	10	0.25	2000	1.5	950	3	565	205000	3.37	3.08
GBU75-T0.25-L2500-S1200-G0.5	75	20	10	0.25	2500	1.5	1200	3	565	205000	2.46	2.23
GBU75-T0.25-L3000-S1450-G0.5	75	20	10	0.25	3000	1.5	1450	3	565	205000	1.95	1.72
GBU75-T0.5-L1000-S450-G0.5	75	20	10	0.5	1000	1.5	450	3	565	205000	23.36	21.32
GBU75-T0.5-L1500-S700-G0.5	75	20	10	0.5	1500	1.5	700	3	565	205000	16.57	13.72
GBU75-T0.5-L2000-S950-G0.5	75	20	10	0.5	2000	1.5	950	3	565	205000	9.78	8.52
GBU75-T0.5-L2500-S1200-G0.5	75	20	10	0.5	2500	1.5	1200	3	565	205000	7.34	5.93
GBU75-T0.5-L3000-S1450-G0.5	75	20	10	0.5	3000	1.5	1450	3	565	205000	4.93	4.32
GBU75-T0.75-L1000-S450-G0.5	75	20	10	0.75	1000	1.5	450	3	565	205000	48.05	41.05
GBU75-T0.75-L1500-S700-G0.5	75	20	10	0.75	1500	1.5	700	3	565	205000	25.97	23.34
GBU75-T0.75-L2000-S950-G0.5	75	20	10	0.75	2000	1.5	950	3	565	205000	16.59	14.75
GBU75-T0.75-L2500-S1200-G0.5	75	20	10	0.75	2500	1.5	1200	3	565	205000	11.15	9.95

GBU75-T0.75-L3000-S1450-G0.5	75	20	10	0.75	3000	1.5	1450	3	565	205000	8.18	7.02
GBU75-T1.0-L1000-S450-G0.5	75	20	10	1.0	1000	1.5	450	3	565	205000	65.71	62.00
GBU75-T1.0-L1500-S700-G0.5	75	20	10	1.0	1500	1.5	700	3	565	205000	37.34	34.57
GBU75-T1.0-L2000-S950-G0.5	75	20	10	1.0	2000	1.5	950	3	565	205000	23.29	20.36
GBU75-T1.0-L2500-S1200-G0.5	75	20	10	1.0	2500	1.5	1200	3	565	205000	15.14	13.22
GBU75-T1.0-L3000-S1450-G0.5	75	20	10	1.0	3000	1.5	1450	3	565	205000	10.26	8.97
GBU75-T1.25-L1000-S450-G0.5	75	20	10	1.25	1000	1.5	450	3	565	205000	88.94	75.00
GBU75-T1.25-L1500-S700-G0.5	75	20	10	1.25	1500	1.5	700	3	565	205000	46.74	43.53
GBU75-T1.25-L2000-S950-G0.5	75	20	10	1.25	2000	1.5	950	3	565	205000	28.59	26.34
GBU75-T1.25-L2500-S1200-G0.5	75	20	10	1.25	2500	1.5	1200	3	565	205000	17.99	15.82
GBU75-T1.25-L3000-S1450-G0.5	75	20	10	1.25	3000	1.5	1450	3	565	205000	12.56	10.77
GBU75-T1.5-L1000-S450-G0.5	75	20	10	1.5	1000	1.5	450	3	565	205000	109.37	100.52
GBU75-T1.5-L1500-S700-G0.5	75	20	10	1.5	1500	1.5	700	3	565	205000	55.49	52.36
GBU75-T1.5-L2000-S950-G0.5	75	20	10	1.5	2000	1.5	950	3	565	205000	33.48	30.20
GBU75-T1.5-L2500-S1200-G0.5	75	20	10	1.5	2500	1.5	1200	3	565	205000	20.95	18.51
GBU75-T1.5-L3000-S1450-G0.5	75	20	10	1.5	3000	1.5	1450	3	565	205000	14.68	12.72

Table A.11: Axial capacity obtained from the parametric study results for GBU75-T0.25 to T1.5 with transverse gap (G)= 1.5

Specimen	**Web**	**Flange**	**Lip**	**Thickness**	**Length**	**Fillet radius**	**Spacing**	**Number of spacers**	**Yield Strength**	**Youngs Modulus**	**AS/NZS-4600:2018 (P)**	**FE Results (P FEA)**
	(mm)	(mm)	(mm)	(mm)	(mm)	(mm)	(mm)		(MPa)	(MPa)	(kN)	(kN)
GBU75-T0.25-L1000-S450-G1.5	75	20	10	0.25	1000	1.5	450	3	565	205000	5.47	4.96
GBU75-T0.25-L1500-S700-G1.5	75	20	10	0.25	1500	1.5	700	3	565	205000	4.44	4.68
GBU75-T0.25-L2000-S950-G1.5	75	20	10	0.25	2000	1.5	950	3	565	205000	3.37	3.40
GBU75-T0.25-L2500-S1200-G1.5	75	20	10	0.25	2500	1.5	1200	3	565	205000	2.46	2.56
GBU75-T0.25-L3000-S1450-G1.5	75	20	10	0.25	3000	1.5	1450	3	565	205000	1.95	1.71
GBU75-T0.5-L1000-S450-G1.5	75	20	10	0.5	1000	1.5	450	3	565	205000	23.36	22.11
GBU75-T0.5-L1500-S700-G1.5	75	20	10	0.5	1500	1.5	700	3	565	205000	16.57	16.18
GBU75-T0.5-L2000-S950-G1.5	75	20	10	0.5	2000	1.5	950	3	565	205000	9.78	10.21
GBU75-T0.5-L2500-S1200-G1.5	75	20	10	0.5	2500	1.5	1200	3	565	205000	7.34	7.08

GBU75-T0.5-L3000-S1450-G1.5	75	20	10	0.5	3000	1.5	1450	3	565	205000	4.93	5.09
GBU75-T0.75-L1000-S450-G1.5	75	20	10	0.75	1000	1.5	450	3	565	205000	48.05	46.796
GBU75-T0.75-L1500-S700-G1.5	75	20	10	0.75	1500	1.5	700	3	565	205000	25.97	27.167
GBU75-T0.75-L2000-S950-G1.5	75	20	10	0.75	2000	1.5	950	3	565	205000	16.59	16.57
GBU75-T0.75-L2500-S1200-G1.5	75	20	10	0.75	2500	1.5	1200	3	565	205000	11.15	11.154
GBU75-T0.75-L3000-S1450-G1.5	75	20	10	0.75	3000	1.5	1450	3	565	205000	8.18	8.2
GBU75-T1.0-L1000-S450-G1.5	75	20	10	1.0	1000	1.5	450	3	565	205000	65.71	62.06
GBU75-T1.0-L1500-S700-G1.5	75	20	10	1.0	1500	1.5	700	3	565	205000	37.34	37.68
GBU75-T1.0-L2000-S950-G1.5	75	20	10	1.0	2000	1.5	950	3	565	205000	23.29	24.09
GBU75-T1.0-L2500-S1200-G1.5	75	20	10	1.0	2500	1.5	1200	3	565	205000	15.14	15.80
GBU75-T1.0-L3000-S1450-G1.5	75	20	10	1.0	3000	1.5	1450	3	565	205000	10.26	10.67
GBU75-T1.25-L1000-S450-G1.5	75	20	10	1.25	1000	1.5	450	3	565	205000	88.94	85.45
GBU75-T1.25-L1500-S700-G1.5	75	20	10	1.25	1500	1.5	700	3	565	205000	46.74	48.06
GBU75-T1.25-L2000-S950-G1.5	75	20	10	1.25	2000	1.5	950	3	565	205000	28.59	28.07
GBU75-T1.25-L2500-S1200-G1.5	75	20	10	1.25	2500	1.5	1200	3	565	205000	17.99	18.64
GBU75-T1.25-L3000-S1450-G1.5	75	20	10	1.25	3000	1.5	1450	3	565	205000	12.56	13.05
GBU75-T1.5-L1000-S450-G1.5	75	20	10	1.5	1000	1.5	450	3	565	205000	109.37	103.49
GBU75-T1.5-L1500-S700-G1.5	75	20	10	1.5	1500	1.5	700	3	565	205000	55.49	57.94
GBU75-T1.5-L2000-S950-G1.5	75	20	10	1.5	2000	1.5	950	3	565	205000	33.48	33.36
GBU75-T1.5-L2500-S1200-G1.5	75	20	10	1.5	2500	1.5	1200	3	565	205000	20.95	21.73
GBU75-T1.5-L3000-S1450-G1.5	75	20	10	1.5	3000	1.5	1450	3	565	205000	14.68	15.17

Appendix-B

B-1. Ansys APDL script to develop FEA models:

The below link refers to Ansys APDL scripts used to develop the FEA models with imperfect geometry

Ansys_APDL_Scripting_Divi

B-2. Python Script to create the input files, which generate the FEA Models with imperfect Geometry in Abaqus

```
#This code generates input for ababqus by joining the files. In this code
manually I have removed the
#file that is idle

import subprocess

# List of files to be joined
folder = r'Z:\B2B\GBU-75-transverse-spacing\t-025'
start = 21
end = 21

inp = int(input("Analysis Mehtod Input: 0 for static, 1 for static riks, 2 for
dynamic implicit: "))

if inp == 0:
    file_list = [
        "heading.inp",
        "parts.inp",
        "node_def.inp",
        "CB_W_002nt01.csv",
        "elem_def_1.inp",
        "CB_W_002et01.csv",
        "elem_def_2.inp",
        "CB_W_002et02.csv",
        "nset_disp_uz.inp",
        "CB_W_002disp_uz.csv",
        "nset_ux.inp",
        "CB_W_002nux.csv",
        "nset_uy.inp",
        "CB_W_002nuy.csv",
        "nset_uz.inp",
        "CB_W_002nuz.csv",
        "nset_roty.inp",
        "CB_W_002roty.csv",
        "nset_rotz.inp",
        "CB_W_002rotz.csv",
        "nset_bottom_end.inp",
        "CB_W_002bottom_end.csv",
        "nset_top_end.inp",
        "CB_W_002top_end.csv",
        "CB_W_002MI.inp",
        "shell_section_1.inp",
        "CB_W_002thickness.csv",
        "shell_section_2.inp",
```

```
        "CB_W_002thickness.csv",
        "assembly.inp",
        "CB_W_002UC.inp",
        "material_general.inp",
        "CB_W_002elastic_properties.csv",
        "plastic.inp",
        "CB_W_002general_yield.csv",
        "material_corners.inp",
        "CB_W_002elastic_properties.csv",
        "plastic.inp",
        "CB_W_002corner_yield.csv",
        "boundary.inp",
        "analysis_S.txt",
        "boundary_2.inp",
        "CB_W_002displacement.csv",
        "output.inp"
        ]

    # Folder location for the files
    folder_location = folder

    # Generate the joined input file for each version (There are 15 files to
be joined starting from CB_W_002 t0 CB_W_0015)
    version_start = start
    version_end = end

    for version in range(version_start, version_end + 1):
        if version < 10:
            version_str = str(version).zfill(3)
        elif 10 <= version < 100:
            version_str = str(version).zfill(4)
        else:
            version_str = str(version).zfill(5)

        output_file = f"{version_str}.inp"   #Generation of the abaqus input
files. Here I am getting 15 files for abaqus input that I want to run in batch
mode
        command = ["copy", "/b"]

        for filename in file_list:
            new_filename = filename.replace("CB_W_002", f"CB_W_{version_str}")
            command.extend([f"{folder_location}\\{new_filename}", "+"])

        command.pop()  # Remove the last "+"
        command.append(f"{folder_location}\\{output_file}")

        try:
            subprocess.run(command, shell=True, check=True)
            print(f"Files have been concatenated successfully. Output file:
{output_file}")
        except subprocess.CalledProcessError as e:
            print(f"An error occurred during file concatenation for version
{version}: {e}")
    print("Completed")

elif inp==1:
    file_list = [
        "heading.inp",
        "parts.inp",
        "node_def.inp",
        "CB_W_002nt01.csv",
```

```
        "elem_def_1.inp",
        "CB_W_002et01.csv",
        "elem_def_2.inp",
        "CB_W_002et02.csv",
        "nset_disp_uz.inp",
        "CB_W_002disp_uz.csv",
        "nset_ux.inp",
        "CB_W_002nux.csv",
        "nset_uy.inp",
        "CB_W_002nuy.csv",
        "nset_uz.inp",
        "CB_W_002nuz.csv",
        "nset_roty.inp",
        "CB_W_002roty.csv",
        "nset_rotz.inp",
        "CB_W_002rotz.csv",
        "nset_bottom_end.inp",
        "CB_W_002bottom_end.csv",
        "nset_top_end.inp",
        "CB_W_002top_end.csv",
        "CB_W_002MI.inp",
        "shell_section_1.inp",
        "CB_W_002thickness.csv",
        "shell_section_2.inp",
        "CB_W_002thickness.csv",
        "assembly.inp",
        "CB_W_002UC.inp",
        "material_general.inp",
        "CB_W_002elastic_properties.csv",
        "plastic.inp",
        "CB_W_002general_yield.csv",
        "material_corners.inp",
        "CB_W_002elastic_properties.csv",
        "plastic.inp",
        "CB_W_002corner_yield.csv",
        "boundary.inp",
        "analysis_SR.txt",
        "boundary_2.inp",
        "CB_W_002displacement.csv",
        "output.inp"
        ]

    # Folder location for the files
    folder_location = folder

    # Generate the joined input file for each version (There are 15 files to
be joined starting from CB_W_002 t0 CB_W_0015)
    version_start = start
    version_end = end

    for version in range(version_start, version_end + 1):
        if version < 10:
            version_str = str(version).zfill(3)
        elif 10 <= version < 100:
            version_str = str(version).zfill(4)
        else:
            version_str = str(version).zfill(5)

        output_file = f"{version_str}.inp"   #Generation of the abaqus input
files. Here I am getting 15 files for abaqus input that I want to run in batch
mode
```

```
        command = ["copy", "/b"]

        for filename in file_list:
            new_filename = filename.replace("CB_W_002", f"CB_W_{version_str}")
            command.extend([f"{folder_location}\\{new_filename}", "+"])

        command.pop()  # Remove the last "+"
        command.append(f"{folder_location}\\{output_file}")

        try:
            subprocess.run(command, shell=True, check=True)
            print(f"Files have been concatenated successfully. Output file:
{output_file}")
        except subprocess.CalledProcessError as e:
            print(f"An error occurred during file concatenation for version
{version}: {e}")
    print("Completed")

elif inp==2:
    file_list = [
         "heading.inp",
        "parts.inp",
        "node_def.inp",
        "CB_W_002nt01.csv",
        "elem_def_1.inp",
        "CB_W_002et01.csv",
        "elem_def_2.inp",
        "CB_W_002et02.csv",
        "nset_disp_uz.inp",
        "CB_W_002disp_uz.csv",
        "nset_ux.inp",
        "CB_W_002nux.csv",
        "nset_uy.inp",
        "CB_W_002nuy.csv",
        "nset_uz.inp",
        "CB_W_002nuz.csv",
        "nset_roty.inp",
        "CB_W_002roty.csv",
        "nset_rotz.inp",
        "CB_W_002rotz.csv",
        "nset_bottom_end.inp",
        "CB_W_002bottom_end.csv",
        "nset_top_end.inp",
        "CB_W_002top_end.csv",
        "CB_W_002MI.inp",
        "shell_section_1.inp",
        "CB_W_002thickness.csv",
        "shell_section_2.inp",
        "CB_W_002thickness.csv",
        "assembly.inp",
        "CB_W_002UC.inp",
        "material_general.inp",
        "CB_W_002elastic_properties.csv",
        "plastic.inp",
        "CB_W_002general_yield.csv",
        "material_corners.inp",
        "CB_W_002elastic_properties.csv",
        "plastic.inp",
        "CB_W_002corner_yield.csv",
        "boundary.inp",
        "analysis_SR.txt",
```

```
        "boundary_2.inp",
        "CB_W_002displacement.csv",
        "output.inp"
        ]

    # Folder location for the files
    folder_location = folder

    # Generate the joined input file for each version (There are 15 files to
be joined starting from CB_W_002 t0 CB_W_0015)
    version_start = start
    version_end = end

    for version in range(version_start, version_end + 1):
        if version < 10:
            version_str = str(version).zfill(3)
        elif 10 <= version < 100:
            version_str = str(version).zfill(4)
        else:
            version_str = str(version).zfill(5)

        output_file = f"{version_str}.inp"   #Generation of the abaqus input
files. Here I am getting 15 files for abaqus input that I want to run in batch
mode
        command = ["copy", "/b"]

        for filename in file_list:
            new_filename = filename.replace("CB_W_002", f"CB_W_{version_str}")
            command.extend([f"{folder_location}\\{new_filename}", "+"])

        command.pop()  # Remove the last "+"
        command.append(f"{folder_location}\\{output_file}")

        try:
            subprocess.run(command, shell=True, check=True)
            print(f"Files have been concatenated successfully. Output file:
{output_file}")
        except subprocess.CalledProcessError as e:
            print(f"An error occurred during file concatenation for version
{version}: {e}")
    print("Completed")

else:
    print("Error: Enter among 0,1,2 to choose correct analysis method")
```

B-3. Python Script used to generate batch file for the Abaqus to run in Batch mode:

```
# This code take the ababqus input files and generate the batch file.

# File paths
commands_text_file = r'Z:\B2B\GBU-75-transverse-spacing\t-025\command1.txt'
commands_batch_file = r'Z:\B2B\GBU-75-transverse-spacing\t-025\batch1.bat'

# Range of job numbers
start = 2
end = 20

# Generate the commands text file
with open(commands_text_file, 'w') as file:
    for i in range(start, end + 1):
        if i<10:
            file.write(f'call abaqus job={i:03} cpus=4 int\n')
        elif 10<=i<100:
            file.write(f'call abaqus job={i:04} cpus=4 int\n')
        else:
            file.write(f'call abaqus job={i:05} cpus=4 int\n')

print("Commands text file generated successfully.")

# Convert the text file to a batch file
with open(commands_text_file, 'r') as text_file:
    with open(commands_batch_file, 'w') as batch_file:
        batch_file.write('@echo off\n')
        for line in text_file:
            batch_file.write(line)

print("Batch file created successfully.")
```

B-4. Python Script to tabulate the Maximum Values of Axial Compression strength (kN) in excel file, which helps in creation of curves for different models

```
import re
import openpyxl
import os

folder = r'Z:\B2B\GBU-75-transverse-spacing\t-025'

def extract_maximum_value(file_path):
    max_value = float('-inf')
    read_values = False

    with open(file_path, 'r') as file:
        for line in file:
            line = line.strip()
            if line.startswith('MAXIMUM'):
                max_value_line = re.search(r'MAXIMUM\s+(\d+\.?\d*(?:[Ee][+-
]?\d+)?)', line)
                if max_value_line:
                    max_value = max(max_value, float(max_value_line.group(1)))
            elif line.startswith('NODE'):
```

```
                read_values = True
            elif read_values:
                value_match = re.search(r'\d+\.?\d*(?:[Ee][+-]?\d+)?', line)
                if value_match:
                    value = float(value_match.group())
                    max_value = max(max_value, value)
                else:
                    read_values = False

    return max_value

# Range of files to process
start = 2
end = 21

# Create a new Excel workbook and sheet
wb = openpyxl.Workbook()
sheet = wb.active

# Set the header
sheet.cell(row=1, column=1, value="File")
sheet.cell(row=1, column=2, value="Maximum Value")

# Process each file in the range
for file_num in range(start, end + 1):
    if file_num<10:
        file_path = f'{folder}\\{file_num:03}.dat'
        try:
            max_value = extract_maximum_value(file_path)
        except FileNotFoundError:
            print(f"File {file_path} not found. Skipping.")
            continue
    elif 10<=file_num<100:
        file_path = f'{folder}\\{file_num:04}.dat'
        try:
            max_value = extract_maximum_value(file_path)
        except FileNotFoundError:
            print(f"File {file_path} not found. Skipping.")
            continue
    else:
        file_path = f'{folder}\\{file_num:05}.dat'
        try:
            max_value = extract_maximum_value(file_path)
        except FileNotFoundError:
            print(f"File {file_path} not found. Skipping.")
            continue

    # Write file number and maximum value to Excel
    row = file_num - start + 2
    sheet.cell(row=row, column=1, value=f"{file_num:03}")
    sheet.cell(row=row, column=2, value=max_value/1000)

# Save the workbook
wb.save(f"{folder}\\Compressive_strength.xlsx")
print("Extraction completed and saved to 'Compressive_strength_0.25T.xlsx'.")
```